CHALMERS

Computational fluid dynamics modelling study of the NH3-SCR process in a catalyzed wall-flow filter for diesel vehicles

Master of Science Thesis [Innovative and sustainable chemical engineering]

MIKAELA FLODIN
PIA FLYDÉN

Department of Chemistry and Bioscience
Division of chemical reaction engineering
CHALMERS UNIVERSITY OF TECHNOLOGY
Göteborg, Sweden, 2011

Acknowledgement

This report is a result of a Master's thesis performed by students from the master program Innovative and sustainable chemical engineering at Chalmers university of technology in Gothenburg, Sweden. The thesis has been performed as a collaboration between the Chemical reaction engineering department at Chalmers university of technology and the Energy Department - Laboratory of catalysis and catalytic processes at Politecnico di Milano. The Master's thesis was performed during the spring term 2011 and the main part of the project was carried out at Politecnico di Milano in Milan.

The aim with the project has been to contribute to the development of a catalyzed wall-flow filter where the reduction of particulate matter and NOx in exhaust from diesel engines can be combined into one unit. CFD-simulations have been used to investigate the fluid dynamics in the system.

We would like to thank our professor and examiner Bengt Andersson at Chalmers university of technology for his commitment and feedback during the project. We would also like to thank our supervisors at Politecnico di Milano professor Enrico Tronconi and PhD Silvia Redaelli for their reception, helpfulness and enthusiasm through the working process. A special thanks goes to Love Håkansson at Engineering Data Resources AS in Sandvika, Norway for his unlimited support and guidance in CFD-modeling.

Milan, May 28th, 2011

Mikaela Flodin and Pia Flydén

Abstract

The purpose with this project was to study an after treatment system for diesel exhaust where the reduction of NOx and PM is combined into one unit. DPF technology together with NH_3-SCR technology is used in order to achieve the reduction. The main purpose with the project was to understand the fluid-dynamics, transport and catalyzed phenomena regulating the behavior of small core samples of catalyzed wall flow-filters and monoliths published in the literature. Further was the purpose to investigate if the results from the laboratory scale can be transferred to a full scale system. To be able to understand the above mentioned phenomena CFD-simulations (computational fluid dynamics) have been carried out with the software Ansys 12.1 together with the simulation tool Fluent.

Simulations have been performed both for a laboratory- and a full scale configuration with the purpose to study if the results from the laboratory scale are transferable to the full scale. The temperature, permeability and porosity influences on pressure, velocity and conversion of NO have been investigated for the wall-flow filter configuration for different volumetric flow rates. Simulations for both a wall-flow filter configuration and a monolith configuration have been performed to study the differences and similarities in concentration profiles of NO and the conversion of NO.

The results showed that the temperature has an effect on the results. Higher temperature gave higher velocity and static pressure and also the conversion increased with increasing temperature. The permeability has effect on the velocity and pressure profiles, but has a negligible impact on the conversion of NO. Porosity influences can be neglected. The most significant parameter regarding the conversion of NO was the residence time, which is connected to the volumetric flow rate and the volume of catalyst. A high residence time, corresponding to a low volumetric flow, gave a high conversion since the reactants have a longer time to react. At the same residence time the conversion of NO was the same for the wall-flow filter configuration and the monolith configuration. However, a difference in the conversion of NO was observed between the full scale and the laboratory scale. When the same residence time was used for the two scales the full scale had a higher conversion of NO compared to the laboratory scale. This was due to the mass transfer resistance caused by the diffusion limitations in the non-flow-through walls in the laboratory scale.

The comparison between the full scale and laboratory scale showed that the main difference that needs to be considered is the ratio between inlet and outlet channels, the volume of catalyst and the non-flow-through walls which are present in the laboratory scale. For the full scale the ratio between the in-and outlet channels is 1/1 while the ratio for the laboratory scale is 4/9. The full scale has a lower volume of catalyst per inlet channel than the laboratory scale.

The conclusion drawn from this project was that caution must be taken if the results from the laboratory scale should be transferred to the full scale. The absolute values for the velocity and pressure are difficult to compare due to the different numbers of in-and outlet channels. To have the conversion measured on the same basis it is not possible to feed the two scales with the same volumetric flow in total or per inlet channel. An adjustment must be made so the feed is the same per volume catalyst; meaning the same residence time for the two scales. Mass transport resistance due to diffusion limitation was observed in the non-flow-through walls in the laboratory which underestimate the NO conversion compared to the full scale.

Contents

1. Introduction

Emissions of polluting particulate matter (PM) and nitrogen oxides affect both the environment and human health, and due to human activity the amount of these emissions has drastically increased. It is known that particles in the range of 10 nm to 10 µm have negative effects on human health due to that these particles can be trapped in the respiratory system causing an increased risk of several lung diseases. Emissions of nitrogen oxides contribute to acidification, eutrophication and formation of ground level ozone. Especially in urban areas the emissions of particulate matter and nitrogen oxides are significant, and studies have shown that diesel engines are largely responsible for these emissions. It is therefore of high interest to design diesel engines in a way that makes it possible to reduce these emissions. [1]

1.1 Background

Generally there are two ways to reduce particulate matter from exhaust gas from diesel engines; either by optimizing the fuel combustion or by using an after treatment system where the exhaust gas is filtered. Also when it comes to reduction of nitrogen oxides there are mainly two different strategies; either primary actions where a modification in the air supply is made, or secondary actions where the exhaust reacts with i.e ammonia to form water and nitrogen. The secondary action used in the automotive industry is SCR (Selective Catalytic Reduction).

The emission limits for diesel engines are expected to be further reduced in the future, and therefore it will be a challenge to pack both a large volume of SCR catalyst and diesel particulate filter (DPF) into the engine. To be able to reduce the total volume of the cleaning system a device where these two technologies are combined into one unit is of interest. One suggested method is to combine the SCR and DPF technologies by coating the filters with a SCR catalyst. If the two technologies can be combined into one unit it would not only be possible to install it in trucks, but also in cars. Additionally, since the volume of the devise can be reduced it would also be possible to reduce the fuel consumption and thus the CO_2 emissions. So far the research in this area is very limited, however there are some studies where mainly SCR performances of monoliths and wall-flow filters are reported, but the evaluation with experimental data is not satisfactory.

In a previous Master's thesis at Politecnico di Milano the SCR performances of catalyzed DPF samples were investigated. The configuration being used had four inlet channels and nine outlet channels. The results showed that it was uncertainties concerning the overall number of catalyzed walls that effectively participated in the SCR reactions. Another result that was observed was an unexpected limitation in the NO reduction at higher temperatures. A first step to use fluid-dynamic modeling with COMSOL was also taken. However, the results from the fluid-dynamic modeling were not satisfactory and were not consistent with the experimental results.[2]

1.2 Purpose

In this Master's thesis an after treatment system for diesel exhaust where the reduction of NO and PM is combined into one unit will be studied. DPF technology together with NH_3-SCR technology is used in order to achieve the reduction. The main purpose with the project is to understand the fluid-dynamics, transport and catalyzed phenomena regulating the behavior of the small core samples of catalyzed wall-flow filters and monoliths being tested at Politecnico

di Milano. To be able to understand the above mentioned phenomena, CFD-simulations (computational fluid dynamics) will be carried out with the software Ansys 12.1 together with the simulation tool Fluent.

Simulations will be performed both for a laboratory scale, which is published in the literature, and a full scale configuration with the purpose to study if the results from laboratory scale are transferable to the full-scale.

1.3 Constrains

The main purpose of the present project is to understand the fluid dynamics and not to study the reaction network and the mechanisms in the SCR reaction. Therefore will focus will be on the well known standard SCR reaction.

2. Theory

In this section the NH_3-SCR cleaning system is described together with the SCR reactions and the solving methodology in Fluent.

2.1 Description of the NH_3-SCR cleaning system

The NH_3-SCR cleaning system is placed after the engine in the car, but before the exhaust pipe. The location can be seen in figure 1. The exhaust is transported from the engine to the NH_3-SCR cleaning system where the DPF and catalyst is combined. The cleaned exhaust is thereafter transported through the exhaust pipe and out of the system.

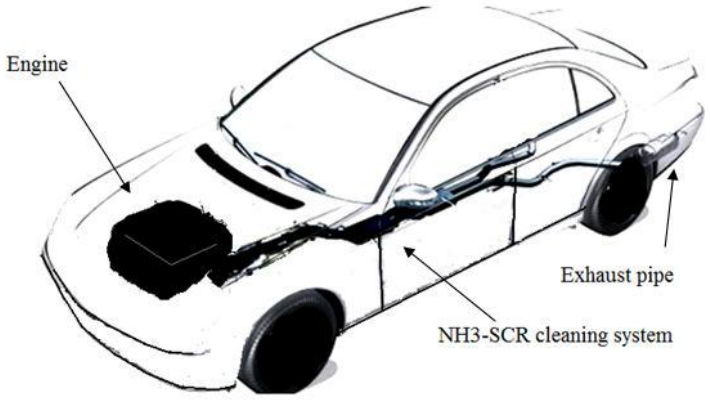

Figure 1. The position of the NH_3-SCR cleaning system in a car.

There are different approaches used to study the NH_3-SCR activity in a catalyzed wall-flow DPF, two often used arrangements are filter system and monolith system. The filter and monolith configurations are consisting of a flow trough device system divided into channels; the wall-flow filter configuration is shown in figure 2. The wall that separates the channels is a porous wall where the catalyst is positioned. In a monolith system the flow enters the channels in the inlet section, flows through the channels and leaves the system in the outlet section. In a filter system every other channel edges are plugged. With this configuration the

flow enters the inlet channels in the inlet section then the flow is forced trough the wall where the catalyst and DPF are located and leaves the system through the outlet channels in the outlet section. Figure 3 shows the difference between the monolith and wall-flow configuration. [3]

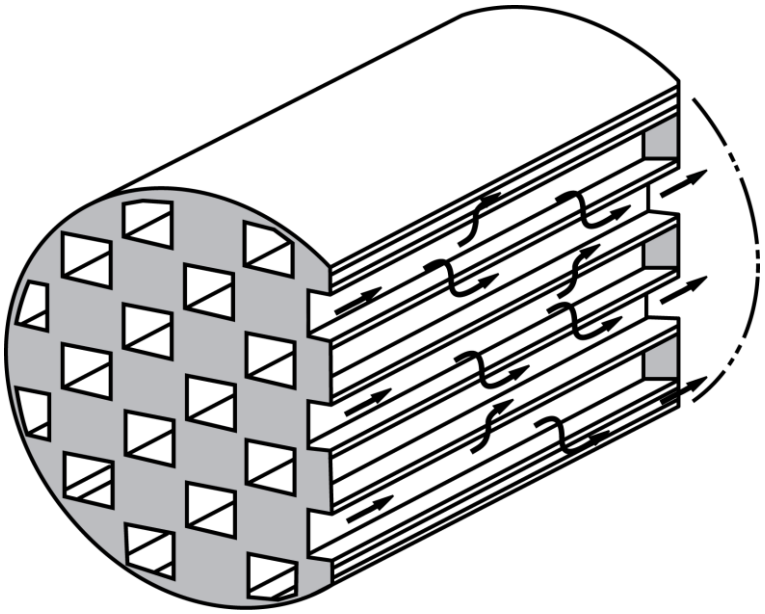

Figure 2. Wall-flow filter device system.

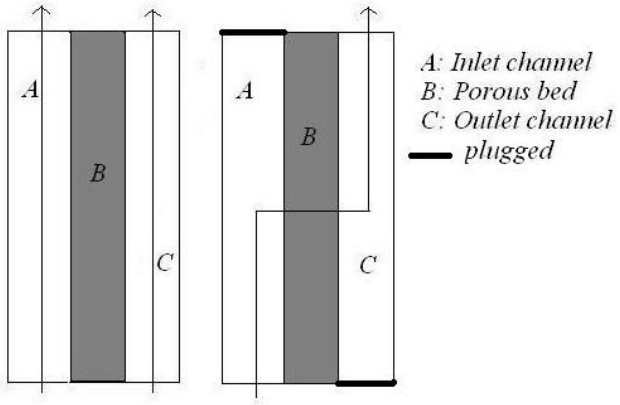

Figure 3. The direction of the flow through the monolith channels (left) and the wall-flow filter channels (right).

The ratio between flow-through walls and non-flow-through walls can be an important factor both in a filter and monolith system. A flow-through wall is a wall where the flow can pass through the porous wall without being stopped by a cement wall. A non-flow-through wall is located beside a cement wall which means that the flow cannot pass through the wall with forced convection but only due to diffusion, figure 4.

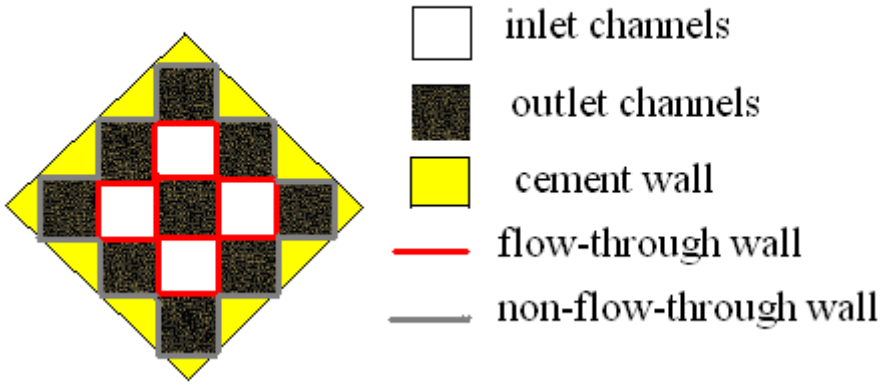

Figure 4. The inlet section of the catalyzed wall-flow filter system. The red lines indicate the flow-through walls and the gray lines the non-flow-through walls.

2.2 Theoretical velocity profile

The velocity profile for a fully developed and laminar flow for squared channels, in a monolith system can theoretically be calculated by equation (1) [4]. The parameters are describes in appendix A. For a wall-flow filter system there is no analytical solution for the velocity profile.

(1)

2.3 Reactions

The idea with the SCR technique is to convert nitrogen oxides to nitrogen and water with the aid of a catalyst. A reductant, usually ammonia or urea, is added to the exhaust gas and absorbs on the catalyst. Nine reactions are needed to be able to describe the entire reaction system when using the SCR technique.

Ammonia adsorption-desorption

[1]

[2]

Ammonia oxidation

[3]

NO oxidation

[4]

Standard SCR

[5]

Ammonium nitrate formation

[6]

NO_2 SCR reaction

[7]

N_2O formation from NO_2 and NH_3

[8]

Fast SCR reaction

[9]

Each reaction has a corresponding reaction rate which is function of the temperature, pressure and concentration of the considered species. The well documented standard SCR reaction's catalytic kinetics can be described by a first-order rate expression in the NO concentration.

2.4. Mass transport resistance

In some cases the rate of physical transport of reactants or heat is lower compared to the rate of the chemical reaction; in that case the reaction is controlled by the mass transport. Mass transport resistance is divided into internal and external resistance, see figure 5. The mass transfer of reactants is first taking place from the bulk phase to the external surface of the catalyst. In the second stage the reactant diffuses from the catalytic surface through the porous material. In the first stage the external resistance (external diffusion) is important and in the second stage the internal resistance (internal diffusion) is important. The external mass transport resistance occurs through an imaginary stagnant film layer while the internal mass transport resistance occurs inside the porous material. If the mass transport resistance is large the conversion will be lower since the transportation in to the porous material where the reaction occurs is very slow compared to the reaction rate.

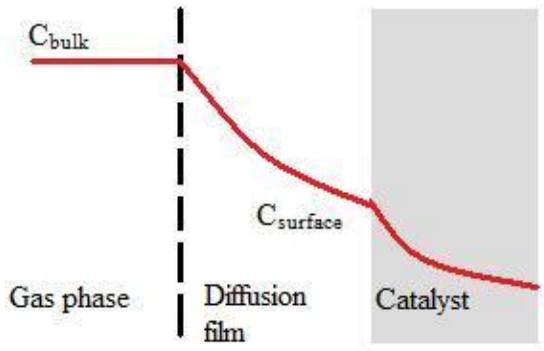

Figure 5. The concentration profile in a bulk phase and a catalytic material, with external and internal resistances.

2.4.1. Thiele modulus and effectiveness factor

The Thiele module is the ratio between the maximum reaction rate and the maximum diffusion rate on a catalyst surface. A large value of the Thiele modulus indicates that the diffusion rate is the limiting factor while a small value indicates that the surface reaction rate is the limiting factor. When the value is below 1 there is no mass transport resistance due to diffusion limitation. When the value is above 3 the reaction is limited by the diffusion rate. For values between 1 and 3 the diffusion starts to have a significant affect. The Thiele module for a first order reaction in slab is calculated with equation (2), the parameters are explained in appendix A:

(2)

Where and (3)

[m^2/s] (4)

The effectiveness factor indicates the extent of diffusion control and is the ratio between the observed overall reaction rate and the maximum rate if the entire interior surface of catalyst is exposed to the surface concentration of the reactant. The effectiveness factor for the above Thiele modulus can be calculated with equation (5), the parameters are explained in appendix A:

[%] (5)

2.5 Fluent

In Fluent a 3D-system is modeled by solving the momentum, mass and energy balance equations for each computational cell equation (6) and the mass and energy equations (7) and (8). The Navier-Stokes is solved during every iteration. For a laminar flow the equation can be solved directly while there is need of approximations for a turbulent flow. Different

turbulence models are available for simplifications and they can either be based on the turbulent viscosity hypothesis or use modeling of the stress tensors.

Navier-Stokes equations (momentum balances):

(6)

Where i and j equals 1, 2, 3 for a 3D-problem

Mass balance:

(7)

Energy balance:

(8)

The source terms in equations (7) and (8) cannot be solved in Fluent since the catalytic reactions occur inside the catalyst walls and these walls are too small to be fully resolved in calculations in Fluent. To solve this problem a user defined function (UDF) is used, see section (2.4.1). [5]

To be able to model for a porous media a momentum source term must be added to the standard fluid flow equations. The source term consists of a viscous loss term part, Darcy's law, and an inertial loss term, equation (9).

(9)

S_i is the source term for the i^{th} (x, y or z) momentum equation, |v| is the magnitude of the velocity, D and C are diagonal matrices. D has 1/ α on the diagonal, where α is the permeability and C has C_2 on the diagonal which is the inertial resistance factor; the other elements are zero. The source term is a contributing factor to the pressure gradient in the porous cell, which creates a pressure drop proportional to the fluid velocity in the cell.

For a case with simple homogeneous porous media equation (10) is used.

(10)

In laminar flows through porous media the pressure drop is usually proportional to velocity and the constant C_2 can be considered as zero. If the non linear effects i.e. convective

acceleration and diffusion are ignored, the porous media model reduces to Darcy's law, equation (11).

– [Pa] (11)

The pressure drop calculated in Fluent is calculated for each of the three coordinate directions, x-, y- and z-direction, equation (12).

—

— (12)

—

$1/\alpha_{ij}$ are the terms in the D matrix in equation (3), v_j is the velocity components in the coordinate directions and are the thickness of the medium in the three directions.

2.5.1 User define function

A UDF is a function programmed by the user that is linked to the solver, i.e. Fluent, to perform certain operations like special boundary conditions, material properties or reaction rates. A UDF can improve the standard functions of the code. Fluent can handle simple reaction rates but when more complex reaction systems are used is it advantageous to use a UDF. The UDF is calculating the reaction rates for each computational cell and sending the information back to Fluent.

In many cases there are different zones in the geometry which have different properties. By using a unique ID for each zone the zones can be identified in the UDF which makes it possible to specify specific properties in specific zones.

2.5.2 Mesh quality

To obtain accurate results a mesh with high quality must be used. The meshing can be made in different ways and the size and shape of the grid can vary. The skewness and the aspect ratio of the computational cell should also be considered. A high skewness of the cell (higher than 0.9 for 3D-problems) can lead to lower accuracy and instability [6]. The aspect ratio of the cell should be less than five, but can be up to 20 if the flow is aligned with grid. Aspect ratio measures the stretching of the cell; a high aspect ratio can lead to an unstable solution which will have trouble to converge. When the meshing is done it is important to handle the grid close to the walls accurate, i.e. adaption can be used to refine the mesh in this region.

2.5.3 Convergence

A reliable convergence criterion is necessary to obtain accurate results. Convergence means that the solution should not change between the iterations and it should be independent of the grid-size. There are different ways for checking convergence, i.e. mass imbalance, scaled residuals and comparison of molar/mass fractions.

Mass imbalance is the amount of mass that is disappearing or added by Fluent during the simulations. A large value (in the same range as the results) indicates that the error is large. The scaled residuals are calculated by Fluent and the absolute convergence criteria for each equation can be chosen so a sufficiently accurate solution is obtained. A low value of the residuals gives a more accurate solution but is more time consuming and difficult. The residuals are an absolute measure of the error.

A comparison of the mass flow in and out of the channels can also be made to study the convergence. The difference between the inflow and outflow should be close to unity to ensure convergence.

3. Modeling approach

The simulations will be divided into two main groups, laboratory scale case and full scale case. They will further be divided into simulations for wall-flow filter system and monolith system with and without reaction. For the laboratory scale, simulations with a reversed channel will also be performed meaning that the outlet section becomes the inlet section and vice versa. Figure 6 shows an overview of the performed simulations. The parameters temperature, velocity, porosity and permeability will be studied in order to see how they influence the pressure and the velocity in the channels and in the porous wall. The NO conversion will be studied and also the concentration of NO in the bulk and on the walls for the cases with reaction.

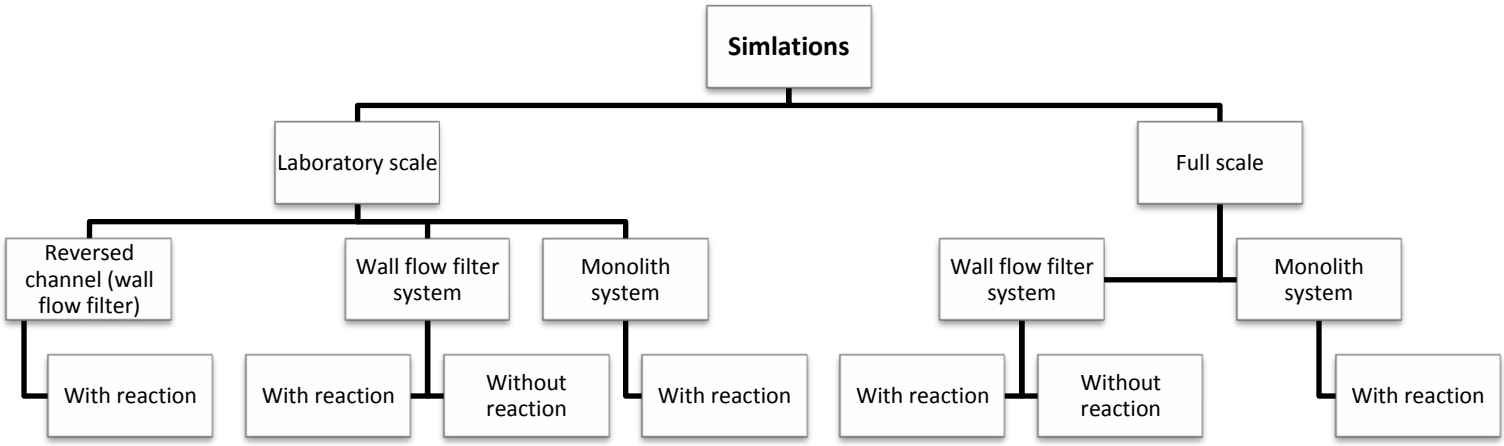

Figure6. An overview of the performed simulations.

In the wall-flow filter system the flow is forced through the porous wall as described in section 2.1. To be able to investigate the effect of forcing the flow through the porous wall a monolith system is modeled as a comparison. The reversed channel with wall-flow filter configuration is simulated to study the influence of the ratio between inlet and outlet channels. In the simulations without reaction only the fluid dynamics of the gas mixture is considered. To investigate not only the fluid dynamics but also the catalyzed phenomena regulating the behavior of the NO-reduction, simulations with reaction are performed. To simplify the

modeling only the standard SCR, reaction, reaction 5, is taken into consideration. The reaction rate for the standard SCR is given in equation 13

— [mol/(m^3, s)] (13)

Where —— (14)

The values for the kinetic parameters are given in appendix B.

3.1 Laboratory scale

For the laboratory scale the inlet and the outlet section of the catalyzed wall-flow filter is shown in figure 7. The inlet section contains four inlet channels and nine closed channels. The inlet channels are open so the flow can enter. The outlet section contains four closed channels and nine outlet channels which are open for the flow to leave the system, figure 7. In the monolith configuration all 13 channels are opened.

In Fluent symmetry planes are used to minimize the geometry needed for modeling. The ratio between the flow-through walls and the non-flow-through walls must be the same in the laboratory scale used during experiments at Politecnico as in the geometry being modeled in Fluent which limits the simplification. The geometry modeled in Fluent is 1/4 of the total volume which detains the ratio between the different walls. The red lines in figure 7 indicate the simulated geometry. All dimensions of the laboratory scale are given in appendix C.

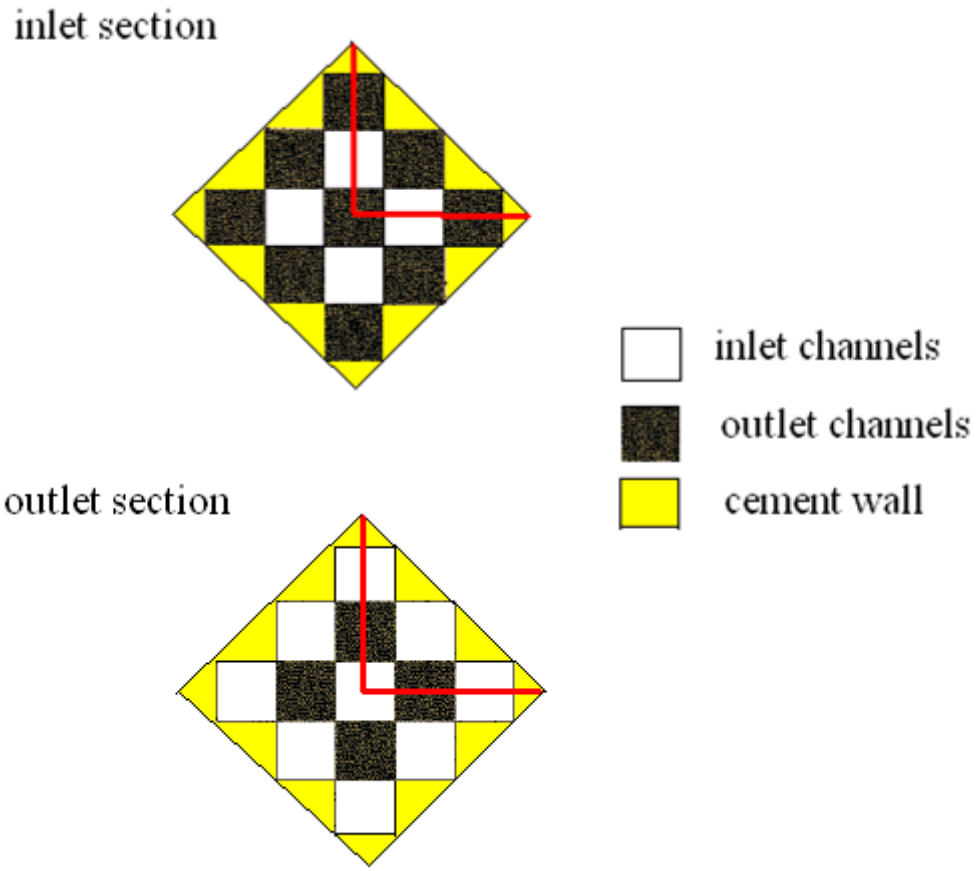

Figure 7. The in- and outlet sections for the configuration used in the laboratory scale. The red lines mark the volume being simulated in Fluent.

To facilitate the discussion about the different channels and porous walls the channels and walls have been named according to figure 8 and figure 9. Channel 10 and 12 in figure 7 are inlet channels and channel 1, 3, 5 and 6 are outlet channels.

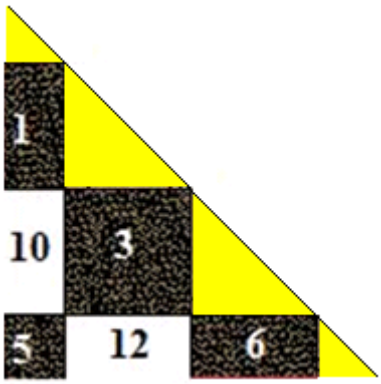

Figure 8. Name selection for the different channels in the laboratory scale viewed from the inlet section.

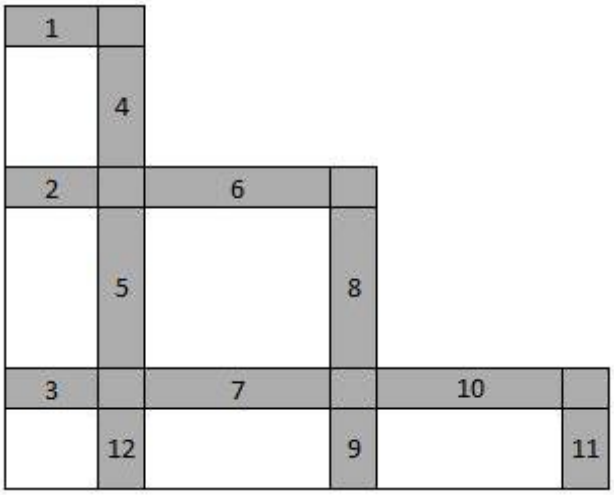

Figure 9. Name selection for the porous walls in the laboratory scale viewed from the inlet section.

In the laboratory scale the non flow-through walls may contribution to the results since the thickness of the catalytic wall the reactant should pass is doubled compared to the thickness in the flow-through walls. In that aspect there might be mass transport resistance in the non-flow-through walls.

To investigate the effect of diffusion limitations the Thiele module and effectiveness factor are calculated at 350 ^{o}C. The Thiele module and effectiveness factor is calculated for both the flow-through walls and the non-flow-through walls for the laboratory scale by using equation (2) and (5).

Where

$[m^2/s]$

This gives the following effectiveness factors:

The value of 0.71 for the Thiele module for the non-flow-through wall indicates that diffusion limitations may occur in these walls in a higher extent compared to the flow-through walls

with the Thiele module 0.36. The different effectiveness factors indicate that there is a difference between the flow-through and the non-flow-through walls.

3.2 Full scale

In the full scale only channels with flow-through walls are considered and thereby no non-flow-through walls are included in the simulations since they are not assumed to have a significant contribution to the result. Symmetry planes are used to minimize the geometry needed for simulations.

For the considered geometry in the full scale the ratio between in- and outlet channels is 1/1 so the inlet section equals the outlet section. The full scale configuration for the catalyzed wall-flow filter is shown in figure 10. Observe that the actual number of in-and outlet channels is not known so the picture does not show any fixed numbers of the in-and outlet channels. The red square indicates the volume being modeled in Fluent. All dimensions of the full scale are given in appendix D.

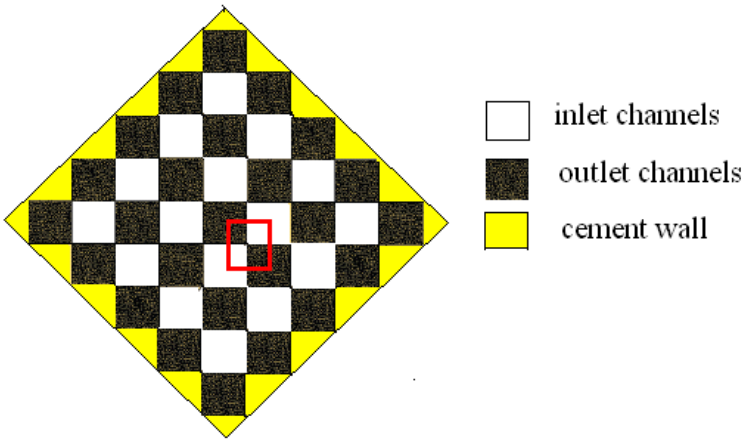

Figure10. The inlet section for the configuration used in the full scale. The red square marks the volume being simulated in Fluent.

To facilitate the discussion about the different channels the channels have been named according to figure 11. Observe that each channel in figure 11 is actually one quarter of the entire channel.

Figure11. Name selection for the different channels in the full scale, viewed from the inlet section.

To investigate the effect of diffusion limitations the Thiele module and effectiveness factor are calculated in the same way as for the flow-through wall in the laboratory scale which gives . and .

The value of 0.36 for the Thiele module indicates that there is not likely to be any mass transport resistance due to diffusion limitations in the walls. The high effectiveness factors combined with the low Thiele module indicates that the surface reaction and not the diffusion is limiting for the full scale system.

3.3. General settings

The general settings are the same for the laboratory scale and the full scale. The feed gas consists of ammonium, nitrogen oxide, water vapor, oxygen and nitrogen. The inlet composition of the gas is given in mass fraction for the different species in table 1. The general information about the both scales is given in table 2.

Table1. Mass fraction of the different species in the inlet flow.

Gas	Mass fraction
NH_3	$2.9464 \cdot 10^{-4}$
NO	$5.1920 \cdot 10^{-4}$
H_2O	0.0312
O_2	0.0886
N_2	inert

Table 2. General information about the full and the laboratory scale.

	Laboratory scale – wall flow	**Laboratory scale – monolith**	**Full scale – wall flow**	**Full scale – monolith**
Channel width [m]	0.001136	0.001136	0.001136	0.001136
Channel length [m]	0.152	0.152	0.152	0.152
Inlet channels	1	4.25	0.5	1
Outlet channels	3.25	4.25	0.5	1
Catalyst load [kg]	$5.877 \cdot 10^{-7}$	$5.877 \cdot 10^{-7}$	$1.306 \cdot 10^{-7}$	$1.306 \cdot 10^{-7}$

The flow velocity, presented in equation 15, is calculated from the normal volumetric flow rate. The volumetric flow rate is converted to velocity in meters per second which is depending on the temperature and number of inlet channels. For the laboratory scale the total normal volumetric flow fed to the system is 4070 Ncm^3/min which gives a volumetric flow per inlet channel of 1017.5 Ncm^3/min.

Calculation of velocity, the parameters are explained in appendix A.

$$\text{———————} \quad [\text{m/s}] \qquad (15)$$

To study the forcing through effect in the wall-flow filter, the monolith system is simulated with the total volumetric flow of 4070 Ncm^3/min which is then divided by 13 inlet channels. For the laboratory scale one simulation with reversed channels at 350 °C is also performed. The total volumetric flow of 4070 Ncm^3/min is then distributed in totally 9 inlets. This simulation is performed to investigate the effects of the ratio between inlets and outlets. The temperatures and velocities for the laboratory scale can be seen in table 3.

Table 3. Temperature and velocity interval for the laboratory scale.

Temperature [^oC]	Velocity [m/s]*	Velocity [m/s]**	Velocity [m/s]***
150	20.3493	6.2613	-
200	22.7538	7.0012	-
250	25.1583	7.7410	-
300	27.5628	8.4809	-
350	29.9673	9.2207	13.3188
400	32.3719	9.9606	-
450	34.7764	10.7004	-
500	37.1809	11.4403	-

* Volumetric flow per inlet channel =1017.5 Ncm^3/min
** Volumetric flow per inlet channel =313.5 Ncm^3/min with monolith system
*** Volumetric flow per inlet channel =452 Ncm^3/min only performed for 350 ^oC

The number of inlet channels is not the same for the laboratory scale and the full scale; this result in different velocity in m/s per inlet channel for the two scales. However, in the first set of simulations the normal volumetric flow per inlet channel will be held constant between the scales meaning that the inlet velocity in each inlet channel in m/s will be the same for the two scales. If the modeled geometry is studied for the laboratory scale and the full scale it can be seen that the volume of catalyst is not the same for the two cases. The laboratory scale has ~4.6 times more volume catalyst than the full scale in the simulated geometry. To be able to have an equal basis to compare the conversion of NO on, additional simulations with an normal volumetric flow of 452 Ncm^3/(min, inlet channel) is performed for the full scale. With this volumetric flow per inlet channel the full scale and laboratory scale will have the same residence time. The monolith simulations are also performed so the residence time for the two scales will be the same which gives a volumetric flow of 225.7 Ncm^3/(min, inlet channel) for the full scale. The temperatures and velocities for the full scale can be seen in table 4.

Table 4. Temperature and velocity interval for the full scale.

Temperature [^{o}C]	Velocity [m/s]*	Velocity [m/s]**	Velocity [m/s]***
150	20.3493	9.0411	4.5139
200	22.7538	10.1128	5.0472
250	25.1583	11.1815	5.5806
300	27.5628	12.2502	6.1139
350	29.9673	13.3188	6.6473
400	32.3719	14.3875	7.1807
450	34.7764	15.4562	7.7140
500	37.1809	16.5248	8.2474

* Volumetric flow per inlet channel =1017.5 Ncm^3/min
**Volumetric flow per inlet channel=452 Ncm^3/min
***Volumetric flow per inlet channel=225.7 Ncm^3/min with monolith system

The volumetric flow rates give rise to different residence times. The residence time is calculated by taking the volume of the porous wall times the catalytic fraction divided by the normal volumetric flow rate. The residence time is then defined at standard conditions meaning that it is not depending on the temperature. The residence time is calculated by equation 16 and is given in table 5 for each volumetric flow rate.

—— [s] (16)

Table 5. The volumetric flow rate per inlet channel and the corresponding residence time.

Volumetric flow [Ncm^3/min, inlet channel]	Residence time [s]
1017.5*	0.0031
452**	0.0031
1017.5**	0.0014

* Laboratory scale
** Full scale

The conversions of NO from the simulations are calculated by using equation 17. The equation is derived from the mass balance over the system. The parameters are explained in appendix A.

———— [%] (17)

For the monolith case the velocity in four points, in a cross sectional plane in one channel is measured. The cross sectional plane and the coordinates of the points can be seen in figure 12. The dotted line represent the total channel and the solid line is the part which being modeled

in Fluent. The points are taken in a cross sectional plane 2 mm from the outlet section at the distance z=0.15 m to insure fully developed flow. The ratio between the velocity in every point and the maximum velocity in the cross sectional plane is calculated. These ratios are compared with the theoretical values for a monolith system, calculated with equation 1. The maximum velocity is located in the center of the channel, at point 5 in figure 12. The other points are calculated relative to this point.

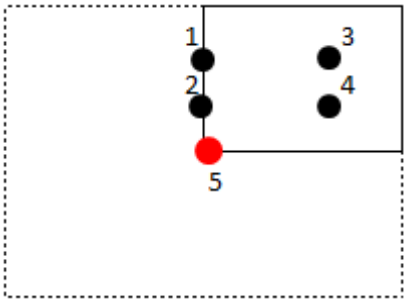

Figure 12. A cross sectional plane in channel 5for laboratory scale and channel 1 in full scale, at z = 0.15 m. The points represent the coordinates where the velocity is measured for a simulated and theoretical monolith system.

Boundary conditions are specified in the inlet, outlet and at the walls. Velocity is defined as the inlet boundary condition and pressure is defined as the outlet boundary condition. On the walls the "no slip" conditions is used. The flow is not considered to be completely developed when it enters the system. Atmospheric pressure and laminar flow are used in the modeling, and a steady-state approach is used.

In all cases the mesh is refined by using adaption. The adaption is done with respect to the gradient of ammonia concentration for the cases with reaction and pressure gradient for the cases without reaction.

3.4 Simulation setup

In the first set of simulations the fluid dynamics is studied with the influence of porosity, permeability and temperature changes for the volumetric flow 1017.5 Ncm^3/(min, inlet channel) for both scales. The conversion of NO is studied for the cases with reaction in the temperature interval 150^{o}C-500^{o}C. In the next set of simulations the conversion is studied in the same temperature interval as mentioned before for the volumetric flow 452 Ncm^3/(min, inlet channel) for the full scale. In the monolith configuration the conversion of NO is studied for the volumetric flow 313.5 Ncm^3/(min, inlet channel) for the laboratory scale and 225.7 Ncm^3/(min, inlet channel) for the full scale. The simulation with the reversed channel is only performed for the laboratory scale at 350 ^{o}C, the used volumetric flow rate is then 452 Ncm^3/(min, inlet channel). The simulation setup can be seen in table 6.

For the laboratory scale with monolith configuration simulations where the mass transport resistance is removed are performed. Two different simulations are performed, one where the internal mass transport resistance is ignored and one where the internal and external mass transport resistance is ignored. The reason for performing these simulations is to investigate the effect of diffusion limitations for the laboratory scale due to the non-flow-through walls. The non-flow-through walls may have significant diffusion limitations which will affect the results of the conversion of NO when comparing with the full scale. The two simulations is

performed at 350 °C with the same volumetric flow as the ordinary monolith simulations, Q = 313.5 Ncm^3/(min, inlet channel). The simulation setup can be seen in table 6.

Table 6. Simulation setup

Running / Variable	1	2	3	4	5	6	7	8	11	12	13	14	15	16	17	18	19	20	21	22	23	24	25	26	27
T=150 ^oC	■															■									
T=200 ^oC		■							■		■		■				■								
T=250 ^oC			■															■							
T=300 ^oC				■															■						
T=350 ^oC					■					■		■		■	■					■				■	■
T=400 ^oC						■															■				
T=450 ^oC							■															■			
T=500 ^oC								■															■		
k = 5.5 •10^{-12} m^2	■	■	■	■	■	■	■	■	■	■	■	■			■	■	■	■	■	■	■	■	■	■	■
k = 5.5 •10^{-13} m^2													■	■											
ε = 0.1 %									■	■															
ε = 0.6 %	■	■	■	■	■	■	■	■					■	■	■	■	■	■	■	■	■	■	■	■	■
ε = 0.99%											■	■													
Wall-flow	■	■	■	■	■	■	■	■	■	■	■	■	■	■	■										
Monolith																■	■	■	■	■	■	■	■	■	■
Reversed channel*															■										
No internal diffusion limitations*																								■	
No internal or external diffusion limitations*																									■

* Only performed for the laboratory scale

4. Result and discussion

In this section is the results presented and discussed for the laboratory scale and the full scale.

4.1 Wall flow filter system with reaction

In this section the results from the wall flow filter case with reaction is shown. The introduction of the reaction did not affect the static pressure and velocity profiles for the laboratory scale nor the full scale. The reason to this is that the amount of reacting species is

low and therefore the temperature will not change do to the reaction. If the temperature does not change the pressure and velocity will not be affected either.

The results are shown for both laboratory and full scale case at 350 °C. The full scale with Q = 1017.5 Ncm3/(min, inlet channel) is presented by the black lines, "—" for inlet and "– -" for outlet. The full scale with Q = 452 Ncm3/(min, inlet channel) is presented by the blue lines, "—" for inlet and "– -" for outlet. The laboratory scale with Q = 1017.5 Ncm3/(min, inlet channel) is presented by the red lines, "- -" for inlet and "– –" for outlet channel 1, "-o-" for channel 3, "-*-" for channel 5 and "-▽-" for channel 6.

4.1.1 Pressure profiles

In figure 13 the pressure profile for in- and outlet channels are shown. The pressure is higher for the full scale with high flow compared to the full scale with low flow and the laboratory scale. In both the in- and outlet channels the static pressure is more than twice as high for the full scale with high flow compare to the laboratory scale. The full scale with low flow has between one third and one half of the static pressure in the laboratory scale. The behavior is the same for the three cases though. In the outlet section the static pressure is decreasing significant and reaching 0 Pa for both the full- and laboratory scale. This behavior is due to the atmospheric pressure in the surrounding. The full scale with high flow has the most significant reduction in the outlet section.

For the laboratory scale the pressure in the two inlet channels is equal since the channels are identical. The outlet channels are not identical and the variations in pressure are therefore expected. Channel 5 has the highest pressure of the outlet channels. This is due to that channel 5 has the lowest pressure drop since all four walls are flow-through walls and therefore the flow can pass through all walls. In channel 1 and 6 which has equal pressure profiles, only one of the four walls is a flow-through wall which causes a higher pressure drop over the porous wall. In channel 3 two of the walls are flow-through walls which results in a pressure profile between the two previously mentioned.

In the full scale all inlet channels are equal and all outlet channels are equal. All walls are flow-through walls so the flow can pass through all walls as soon as it has entered the inlet channels, this result in a low pressure drop over the porous wall. Towards the outlet section the pressure drop increases in the inlet channels because these are plugged while the static pressure in the outlet channels goes down to 0 Pa due to the atmospheric pressure. When Q=1017.5 Ncm^3/(min, inlet channel) the static pressure in the channels is higher compared to when Q=452 Ncm^3/(min, inlet channel) which also results in a higher pressure drop in the outlet section for the higher volumetric flow per inlet channel. Channel 5 in the laboratory scale is the only channel that is comparable with the channels in the full scale, since this is the only channel in the laboratory scale that is surrounded by four flow-through walls. When the same volumetric flow per inlet channel is used for the two scales the static pressure in the outlet channels in the full scale is approximately twice as high as for the laboratory scale.

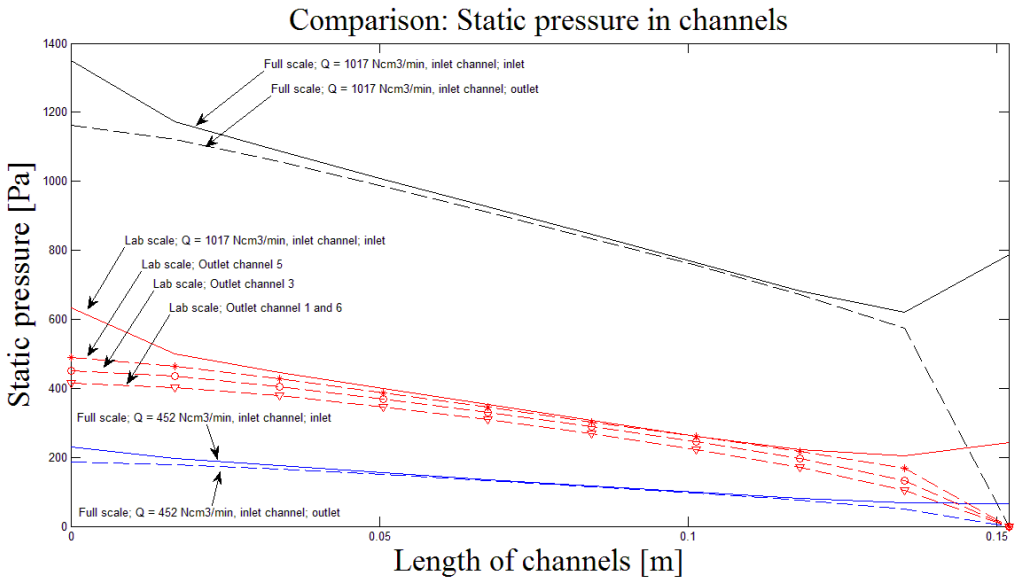

Figure 13. The static pressure along the length of the channels for full scale with Q= 1017.5 Ncm^3/(min, inlet channel), full scale with Q = 452 Ncm^3/(min, inlet channel) and laboratory scale with Q= 1017.5 Ncm^3/(min, inlet channel), wall-flow filter system at 350 °C with reaction.

In figure 14 the pressure through the porous wall is shown. The three cases have rather similar pressure along the length except in the outlet section where the pressure is increasing to a higher value for the full scale with high flow. For the full scale with low flow the static pressure is increasing to a lower value in the outlet section compare to what the static pressure in the laboratory scale does. Full scale with low flow has the lowest pressure drop.

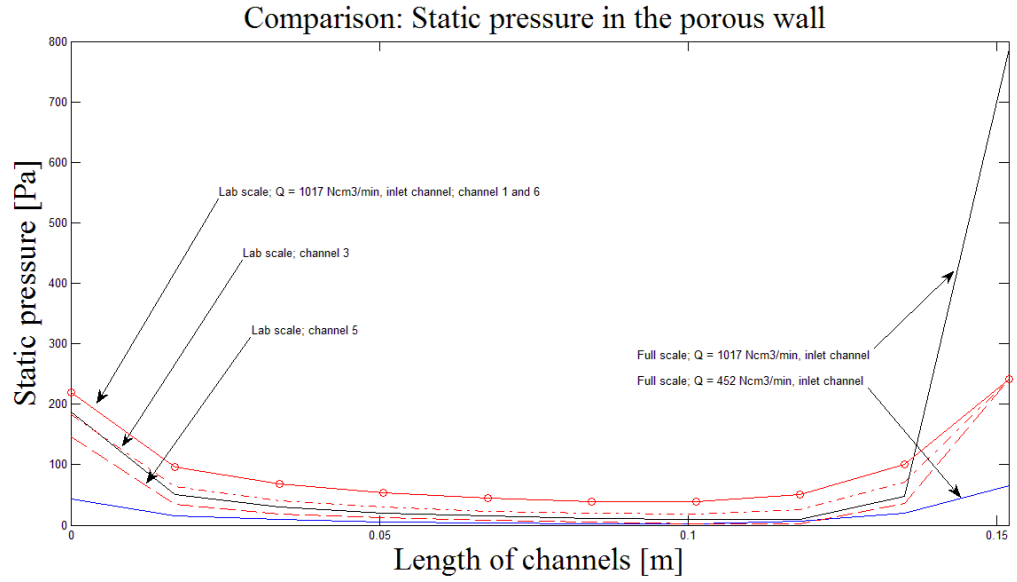

Figure 14. The static pressure drop over the porous wall for full scale with Q= 1017.5 Ncm^3/(min, inlet channel), full scale with Q = 452 Ncm^3/(min, inlet channel) and laboratory scale with Q= 1017.5 Ncm^3/(min, inlet channel) for wall- flow filter system at 350 °C with reaction.

4.1.2 Velocity profiles

In figure 15 and 16 the velocity profiles for in- and outlet channels are shown. The behavior for the three cases is the same; the velocity is decreasing in the inlet channels, and increasing in the outlet channels along the length of the channels. In the inlet channels the full scale with high flow has a higher velocity in the middle of the channels compared to the laboratory scale. The full scale with low flow has a lower velocity, approximately one fifth, compared to the laboratory scale. In the outlet section the velocity for all inlet channels reaches 0 m/s. For the outlet channels the velocity is 0 m/s for all cases in the inlet section.

For the laboratory scale the different velocities are due to different amounts of flow-through walls. The velocity profile in channel 1 and 6 is equal and they have the lowest velocity of the outlet channels. Channel 5 has the highest velocity. Channel 1 and 6 are equal since they have the same number of flow-through walls, one. Channel 3 has two flow-through walls and this will lead to a higher velocity in channel 3 compared to 1 and 6 since the flow has two walls to flow through. Channel 5 has four flow-through walls and will therefore have the highest velocity since the flow can pass through all four porous walls. In the middle of the channels the velocities for the different outlet channels are crossing each other; the reason for this can at the moment not be explained.

For the laboratory scale as well as for the full scale the difference between the in- and outlet channels is highest in the inlet section and in the outlet section of the channels. In the inlet section the flow enters the inlet channels with a given velocity while no flow enters the outlet channels, and this is the reason to the velocity difference in the beginning of the channels. In the outlet section the velocity goes down to 0 m/s in the inlet channels because there is a wall there. The velocity in the outlet channels accelerate due to the increased pressure drop. The profile for the velocity through the porous wall is a result of the pressure drop and therefore these two profiles have the same look. When a lower volumetric flow per inlet channel is used the result is a lower pressure drop and also a lower velocity through the porous wall.

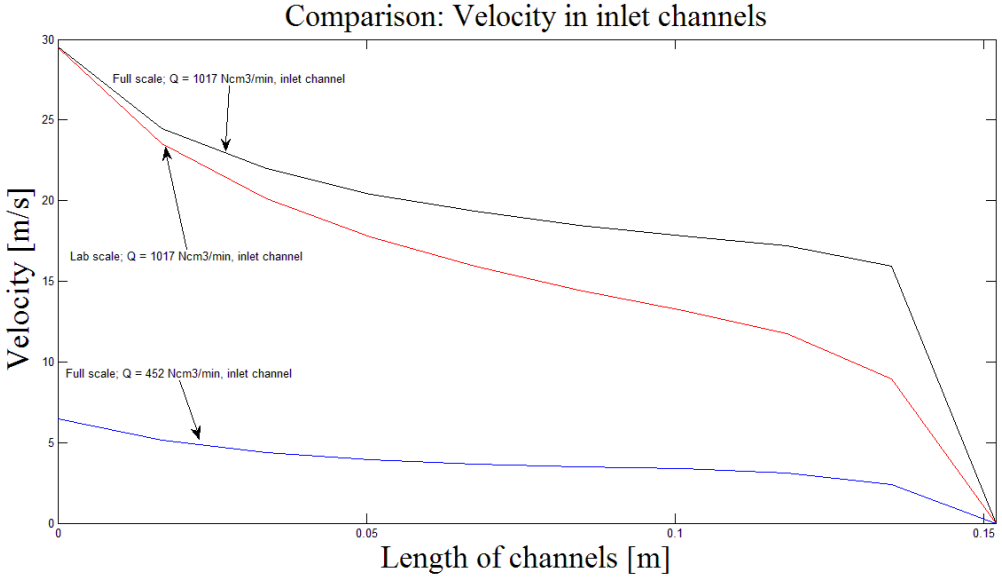

Figure 15. The velocity along the length of the inlet channels for full scale with Q= 1017.5 Ncm^3/(min, inlet channel), full scale with Q = 452 Ncm^3/(min, inlet channel) and laboratory scale with Q= 1017.5 Ncm^3/(min, inlet channel) for wall- flow filter system at 350 °C with reaction.

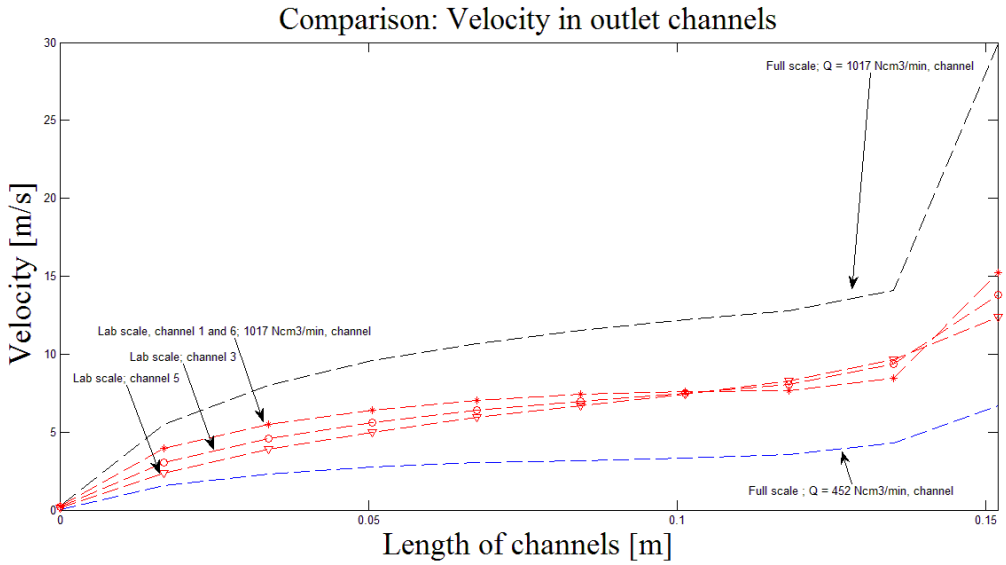

Figure 16. The velocity along the length of the outlet channels for full scale with Q= 1017.5 Ncm^3/(min, inlet channel) , full scale with Q = 452 Ncm^3/(min, inlet channel) and laboratory scale with Q= 1017.5 Ncm^3/(min, inlet channel) for wall- flow filter system at 350 °C with reaction.

When the velocity in the outlet channels is compared for the laboratory scale and the full scale for the same volumetric flow rate per inlet channel it can be noted that the velocity in the outlet section is lower for the laboratory scale than for the full scale which means that the velocity differs in the same way as the static pressure between the two scales do. This behavior can be explained by that the laboratory scale has more outlet channels compared to inlet channels while the full scale has the same number of inlet channels and outlet channels. The same amount of flow is divided between larger amounts of outlet channels in the laboratory scale which is the reason to the reduced velocity. Lower velocity also gives lower static pressure. To confirm this reasoning a simulation for a laboratory scale with a reversed geometry was performed meaning a laboratory scale with more inlet channels compared to outlet channels. The total volumetric flow is the same as before which means that the volumetric flow per inlet channel is lower in the inlet section. The results show that the values for the velocity and the static pressure in the reversed channel are higher compared to the original laboratory scale. The conclusion is that the number of inlet respectively outlet channels is critical for the absolute values for the velocity and static pressure. As long as the number of in- respective outlet channels are not the same for the two scales it is difficult to compare the exact values for static pressure and velocity.

In figure 17 the velocity profiles through the porous wall are shown. The behavior is similar to the pressure drop over the porous wall. The three cases have rather similar velocities along the length except in the outlet section where the velocity is increasing more significant for the full scale with high flow. For the full scale with low flow the velocity is increasing less compare to the laboratory scale.

From the velocity through the porous wall it can be concluded that the velocity is highest towards the end of the channels and lowest in the middle. This means that the contact time between the reactants and the catalyst is higher in the inlet up to the middle of the channel length which gives a more complete reaction.

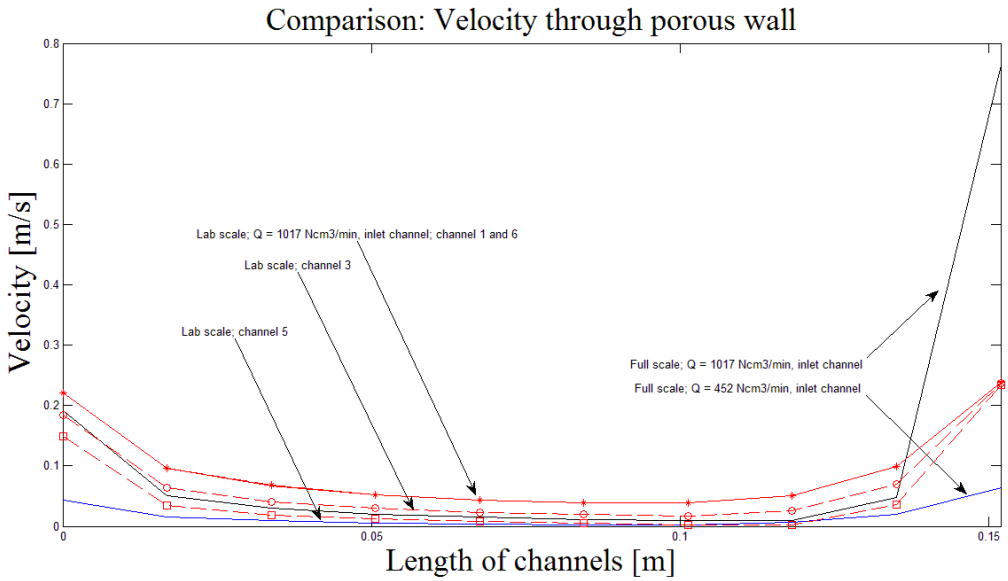

Figure 17. The velocity over the porous wall for full scale with Q= 1017.5 Ncm^3/(min, inlet channel), full scale with Q = 452 Ncm^3/(min, inlet channel) and laboratory scale with Q= 1017.5 Ncm^3/(min, inlet channel), wall- flow filter system at 350 °C with reaction..

4.1.3 Temperature influences

In this section the temperature influence on pressure and velocity is presented for the temperature range 150^{o}C to 500^{o}C. The results are shown for the laboratory scale, but the behavior for the full scale is the same even though the absolute values are not identical due to different volumetric flow rates.

Figure 18 and 19 shows the temperature influence on the static pressure for the in- and outlet channels. The figure shows how the static pressure varies along the length of the channels. When the temperature is increased the static pressure is also increased for both the in- and outlet channels. The static pressure in the inlet channels are affected by the temperature over the entire length. In the outlet channels the temperature has highest effect in the inlet section since the velocity reaches 0 m/s for all temperatures in the outlet section. Figure 20 shows the effect of the temperature on the static pressure drop over the porous wall. The decrease in static pressure and in the beginning and the increase in the end is stronger for the higher temperature compared to the lower. Otherwise the temperature has a low impact on the static pressure drop.

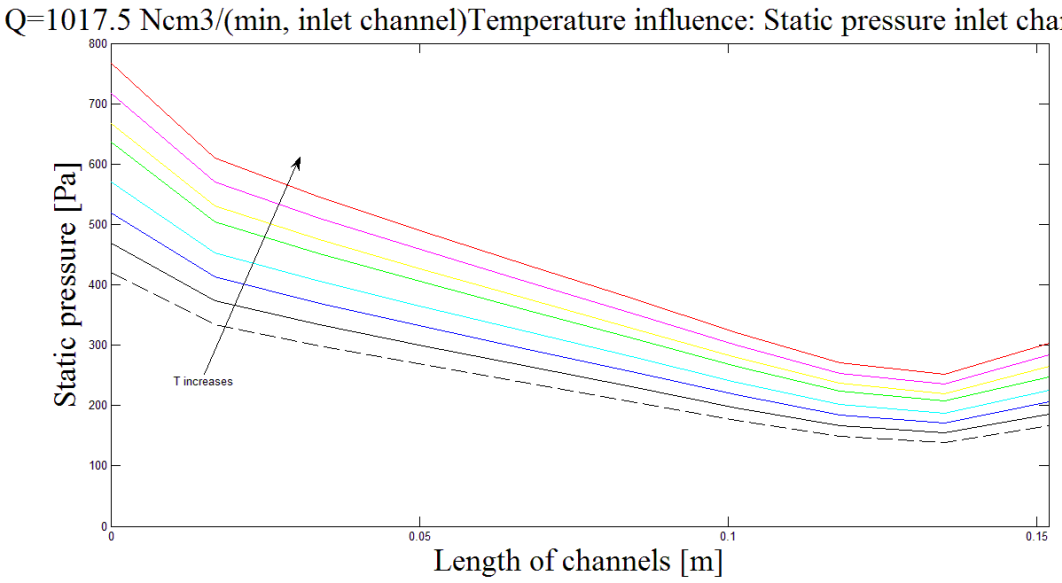

Figure18. The temperature influence on the static pressure in the inlet channel 10 for the laboratory scale wall- flow filter system without reaction and Q = 1017.5 Ncm^3/(min, inlet channel).

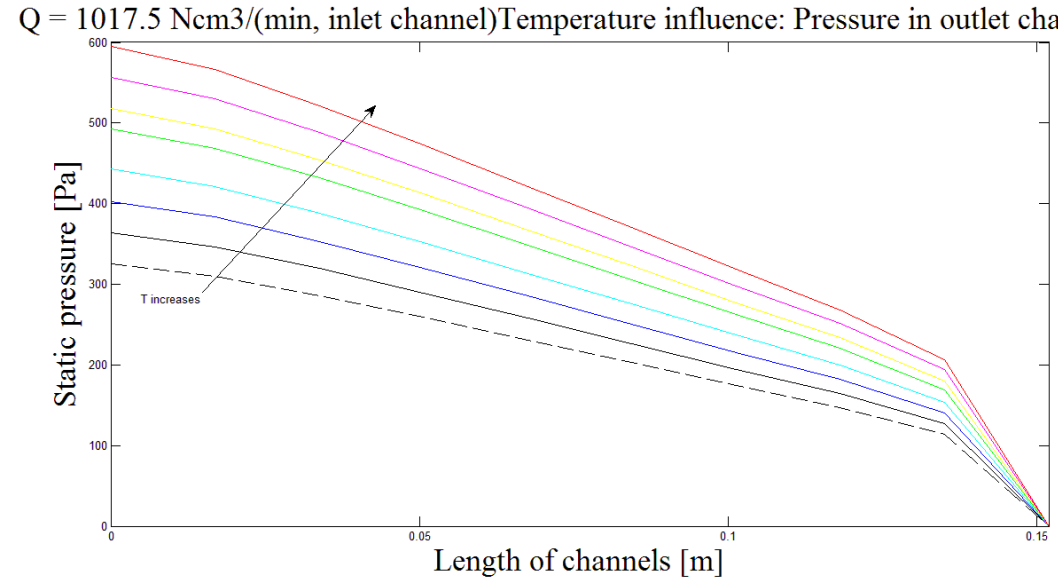

Figure19. The temperature influence on the static pressure in the outlet channels for the laboratory scale wall- flow filter system without reaction and Q = 1017.5 Ncm^3/(min, inlet channel).

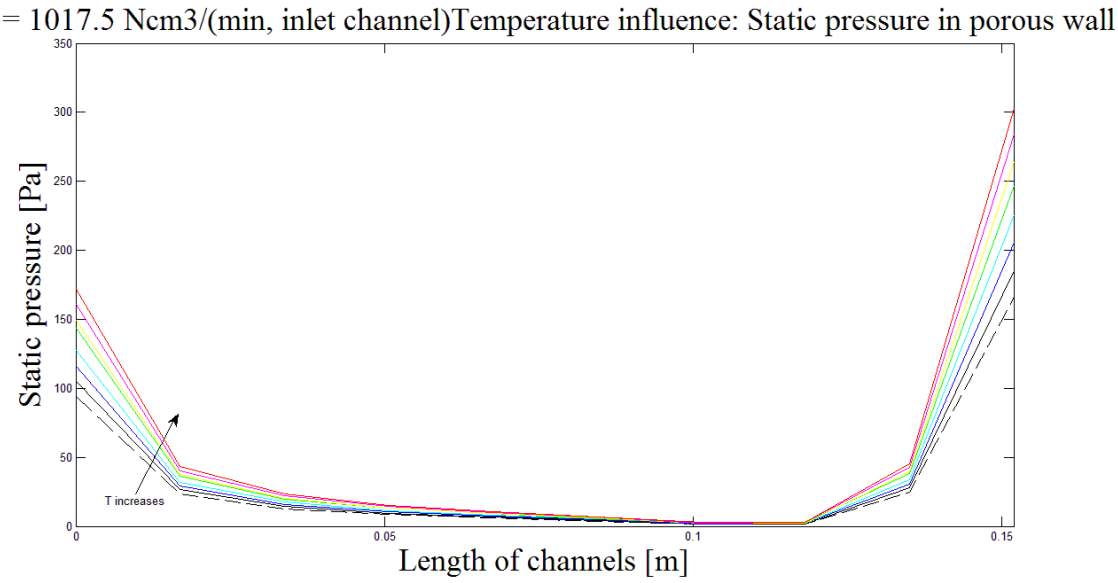

Figure20. The temperature influence on the static pressure drop over the porous wall 12, for the laboratory scale wall- flow filter system without reaction and Q = 1017.5 Ncm^3/(min, inlet channel).

Figure 21, 22 and 23 show the temperature influence on the velocity in the in-and outlet channels and porous wall. A similar behavior as for the static pressure profiles can be noted. The velocity is increasing with increasing temperature for both in-and outlet channels. For the inlet channels the effect of temperature variations is strongest in the inlet section since the velocity reaches 0 m/s for all temperatures in the outlet section. In the outlet channels the temperature effects are strongest in the outlet section. The effects are strongest in the outlet section since the velocity is close to 0 m/s for all temperatures in the inlet section. For the inlet channels the maximum velocity is in the inlet section and for the outlet channels the maximum velocity is in the outlet section. In the porous wall the velocity decreases along the length of the channels and reaches a minimum value before it increases again towards the outlet section. The velocity is increasing with increasing temperature.

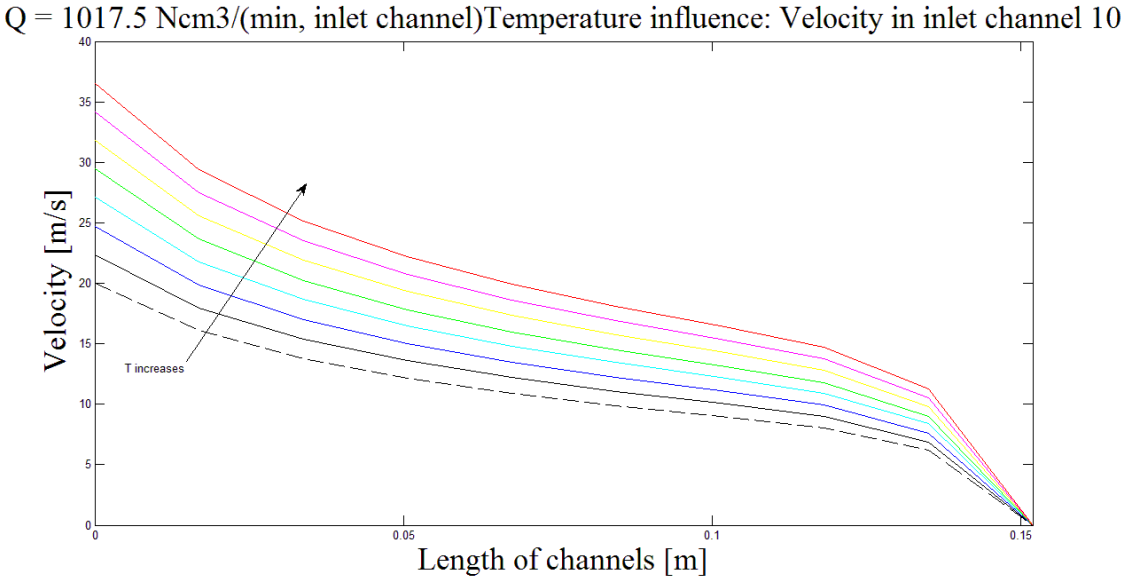

Figure21. The temperature influence on the velocity in the inlet channels for the laboratory scale wall- flow filter system without reaction and Q = 1017.5 Ncm^3/(min, inlet channel).

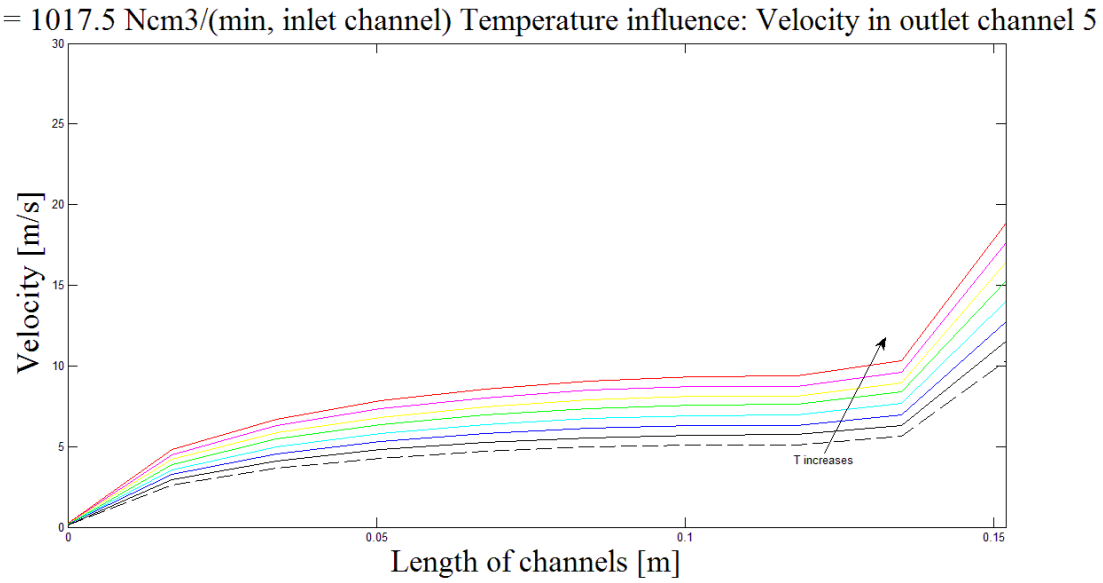

Figure22. The temperature influence on the velocity in the outlet channels for the laboratory scale wall- flow filter system without reaction and Q = 1017.5 Ncm^3/(min, inlet channel).

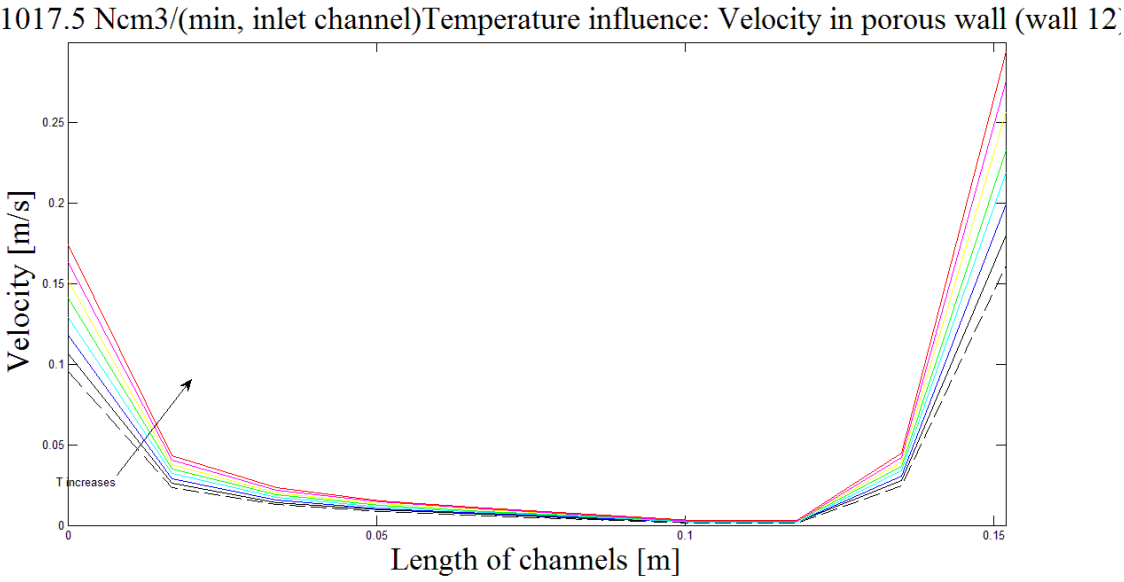

Figure23. The temperature influence on the velocity in porous wall 12 for the laboratory scale wall- flow filter system without reaction and Q = 1017.5 Ncm^3/(min, inlet channel).

Both static pressure and velocity are increasing with increasing temperatures, for inlet and outlet channels. When the temperature increases the gas expands, however if the volume is fixed and there is no space where the gas can expand, the result is that the pressure increases and thereby also the velocity.

4.1.4 Permeability influences

In this section the permeability influence on the static pressure and velocity is presented. The results are shown for the laboratory scale, but the behavior for the full scale is the same even though the absolute values are not identical due to different volumetric flow rates. The

permeability influence is studied for the permeability $5.5\bullet 10^{-12}$ m^2 and $5.5\bullet 10^{-13}$ m^2. The simulations are performed for the temperatures 200 ^oC and 350 ^oC. The permeability $5.5\bullet 10^{-12}$ m^2 is represented with the line "—" and $5.5\bullet 10^{-13}$ m^2 with "- -" in all figures in this section. The results for 350 °C are represented with the red line and the results for 200 °C with the black line.

In figure 24 and 25 the permeability influence on the static pressure in the in- and outlet channels is presented. For the inlet channels the static pressure is approximately twice as large with the low permeability compared to the high permeability. This behavior is found for both temperatures. For the outlet channels the static pressure is larger for the low permeability in the inlet section. In the outlet section the permeability does not have any significant effect on the static pressure since the pressure reaches 0 Pa. The pressure differences due to temperature variations are more significant for the high permeability. Figure 26 shows the pressure drop over the porous wall. The higher permeability gives a lower and more flat pressure drop than the lower permeability. The higher pressure drop in the outlet section with lower permeability is due to that the distribution over the cross section is more uniform is this case.

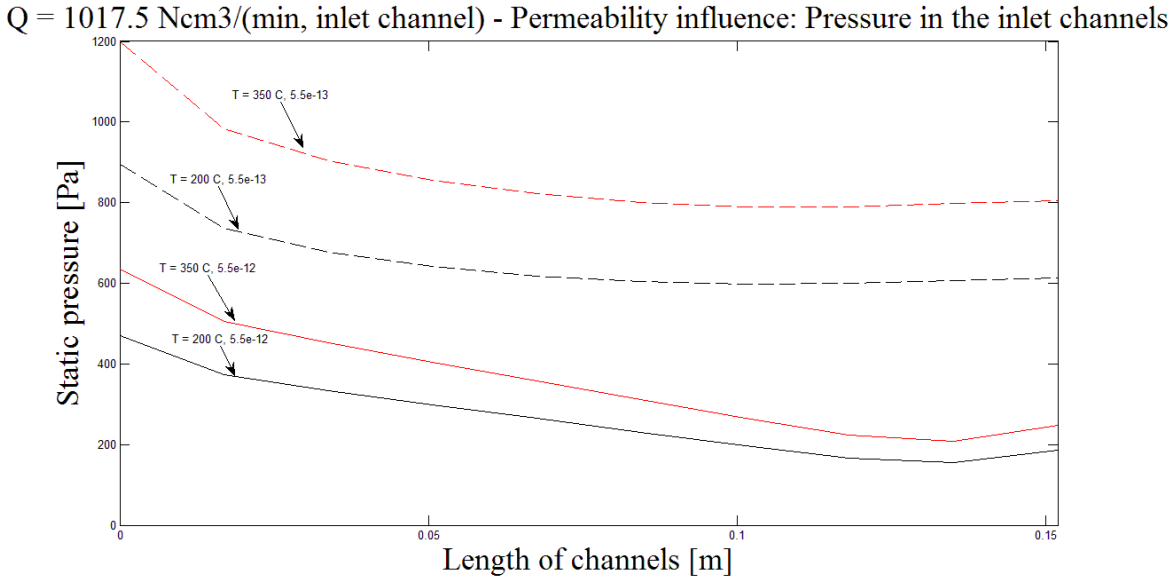

Figure 24. The permeability influence on the static pressure in the inlet channels for the laboratory scale wall- flow filter system with reaction at 200°C and 350 °C and Q = 1017.5 Ncm^3/(min, inlet channel).

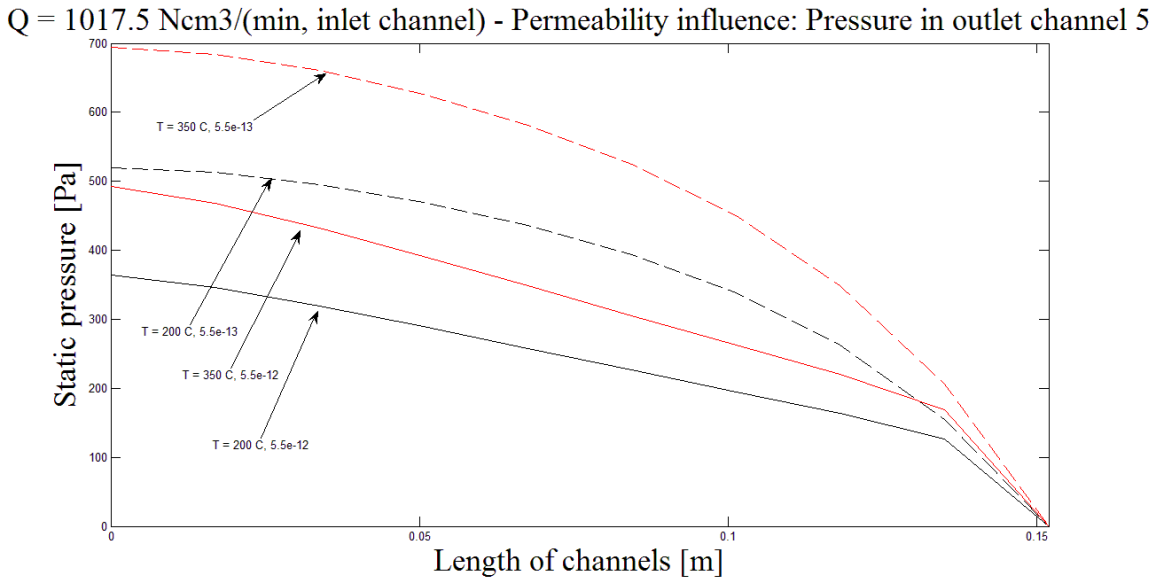

Figure 25. The permeability influence on the static pressure in the outlet channels for the laboratory scale wall- flow filter system with reaction at 200°C and 350 °C and Q = 1017.5 Ncm^3/(min, inlet channel).

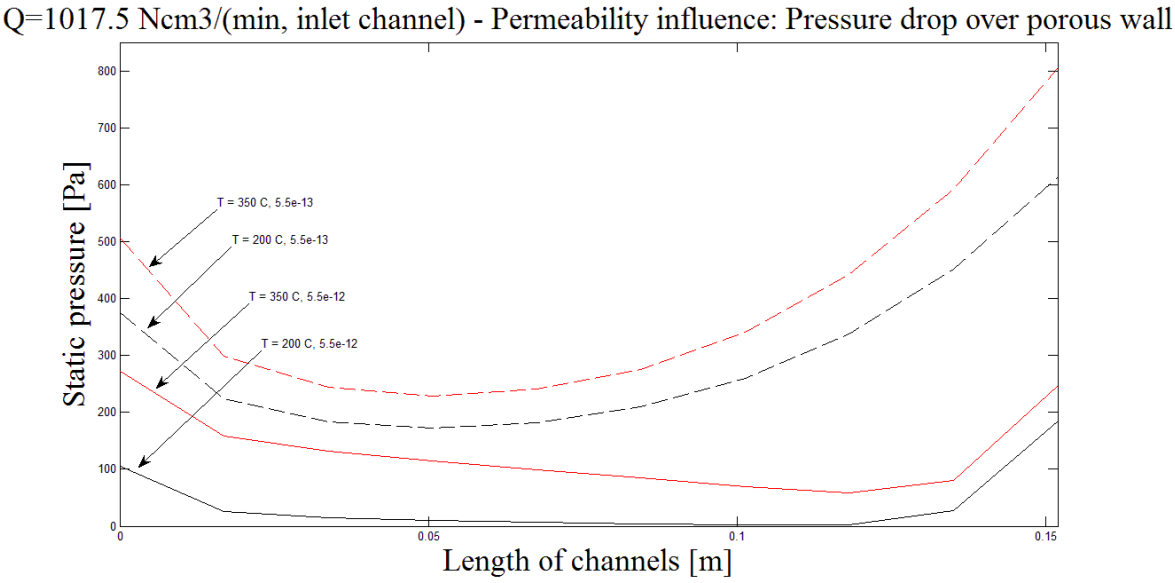

Figure 26. The permeability influence on the static pressure drop over the porous wall for the laboratory scale wall- flow filter system with reaction at 200°C and 350 °C and Q = 1017.5 Ncm^3/(min, inlet channel).

In figure 27 and 28 the permeability influence on the velocity in the in- and outlet channels is presented. For the inlet channels the high permeability gives a more flat velocity profile. In the first half of the channel the low permeability gives a higher velocity compare to the high permeability. In the second half of the channel the low permeability gives a lower velocity. For the outlet channels a high permeability gives a more flat velocity profile compared to the low permeability. In the first half of the channel the low permeability gives a lower velocity compare to the high permeability. In the second half of the channel the low permeability gives a higher velocity.

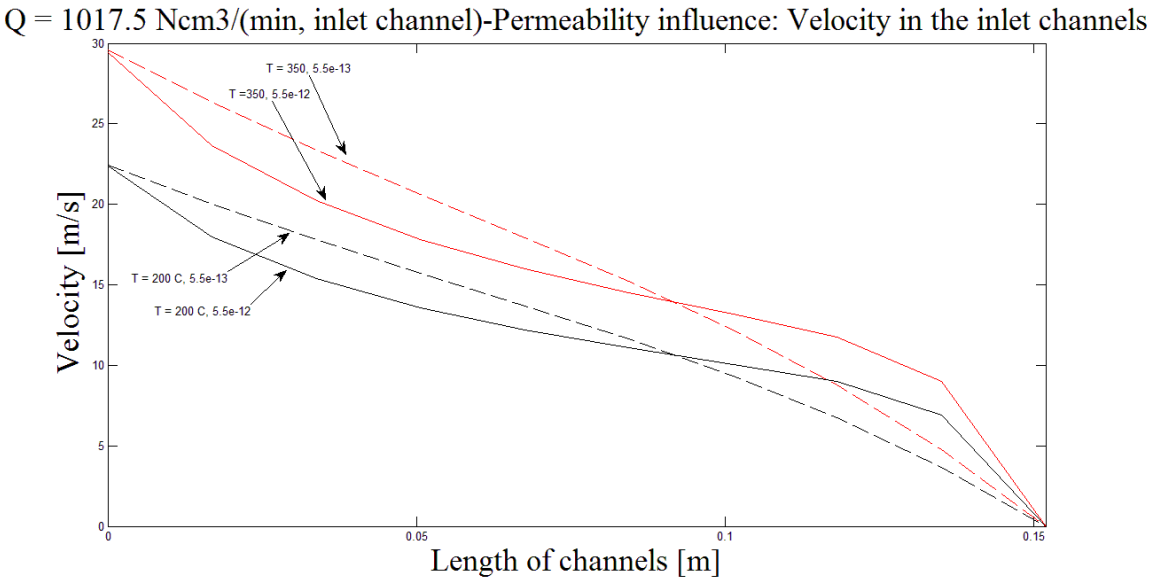

Figure 27. The permeability influence on the velocity in the inlet channels for the laboratory scale wall-flow filter system with reaction at 200°C and 350 °C and Q = 1017.5 Ncm^3/(min, inlet channel).

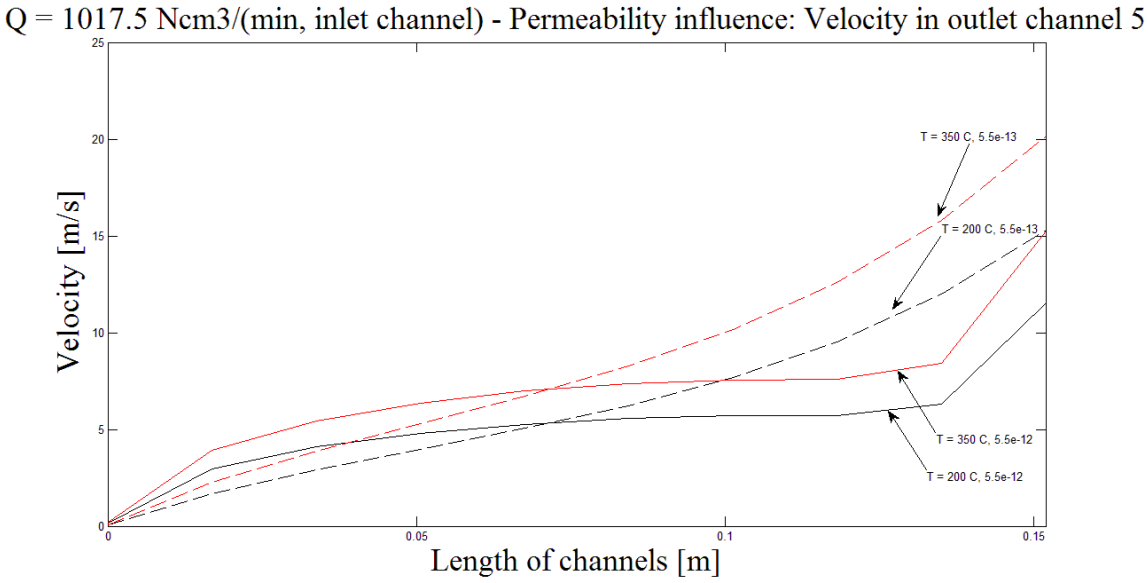

Figure 28. The permeability influence on the velocity in the outlet channels for the laboratory scale wall-flow filter system with reaction at 200°C and 350 °C and Q = 1017.5 Ncm^3/(min, inlet channel).

In figure 29 the permeability influence on the velocity in the porous wall is presented. For the low permeability the velocity has a more flat profile. For the high permeability the velocity has a minimum value in the middle of the channels.

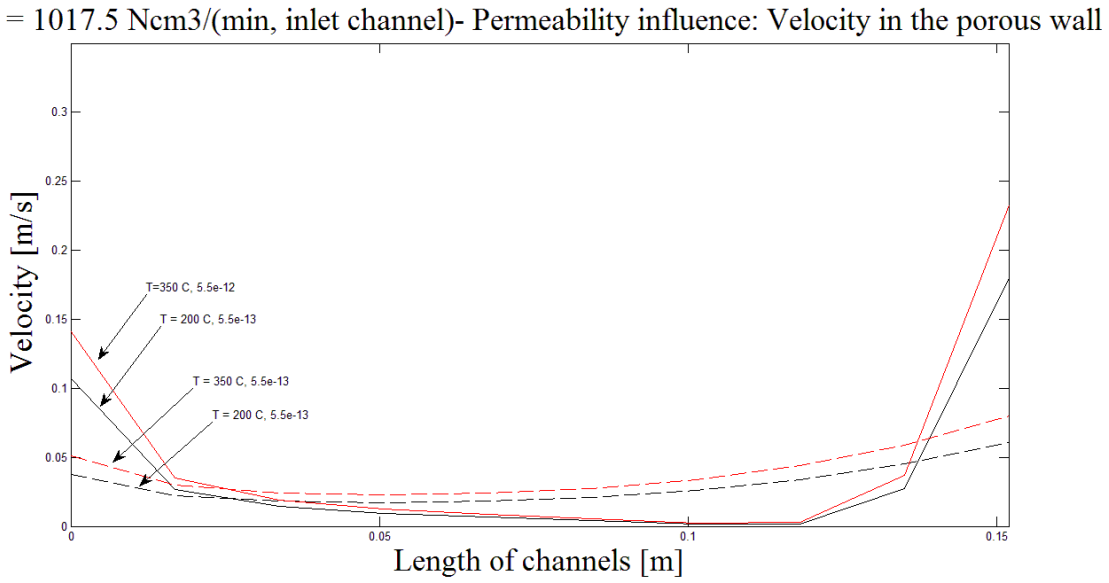

Figure 29. The permeability influence on the velocity in the porous wall for the laboratory scale wall-flow filter system with reaction at 200°C and 350 °C and Q = 1017.5 Ncm^3/(min, inlet channel).

The results show that the permeability has an effect on both the static pressure and velocity. The permeability is included in the denominator in Darcy's law which is used for modeling the porous media, equation (11). Since the permeability is the denominator a low permeability results in a higher pressure drop which is also confirmed by the results.

As was discussed before, the velocity through the porous wall accelerate towards the outlet section. However, when a lower permeability is used the velocity acceleration towards the end of the channels is not that significant. This result indicates that for a lower permeability the distribution of the catalyst is of less importance compared to when a higher value of the permeability is used.

When the conversion of NO was studied for the two different permeabilities a negligible difference in the reduction was observed. This indicates that the way the reactants contact the catalytic material is of minor importance.

4.1.5 Porosity influences

When the porosity influence was studied it was concluded that this parameter has a negligible effect on the results for both the laboratory- and full scale. The porosity does not taking part in the Darcy's law and therefore it is reasonable that the porosity does not have an influence on the results.

4.1.6 Molar fraction of NO

In this section the molar fraction of NO in the bulk and at the surfaces in ppm along the length of the channels is shown for the laboratory scale and the full scale.

4.1.6.1 Laboratory scale

Figure 30 shows the contour plot of the molar concentration of NO for all channels in the outlet section in the laboratory scale. The plot shows the distribution of NO in the different channels. The channel at the top is channel 1. The concentration of NO is highest at the floor and is decreasing towards the roof with a minimum in the upper right corner. The channel to the right on the second level is channel 3. The concentration of NO is homogeneous distributed from the left wall and floor with a minimum concentration in the upper right corner. The lowest concentration is therefore on the roof and right wall. In channel 5, placed to the left on the ground level, the flow is homogeneous distributed from the roof and right wall. The concentration decreases homogeneously towards the lower left corner. Channel 6, placed to the right on the ground level, is equal to channel 1. The concentration is highest at the left wall and is decreasing towards the right wall with a minimum in the upper right corner. The channel to the left on the second level and the one in the middle on the ground level are inlet channels.

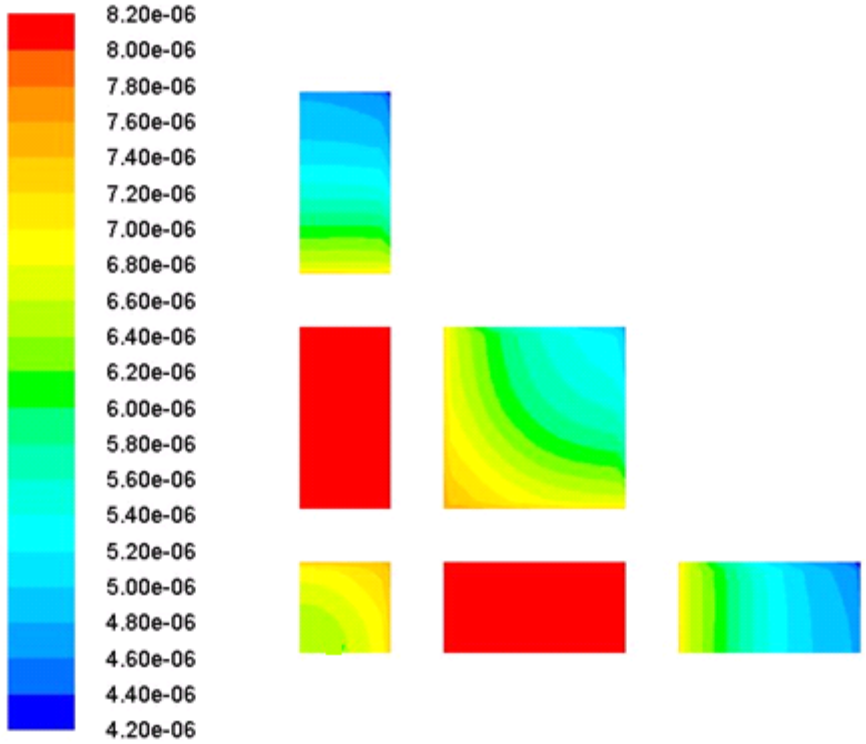

Figure 30. The contours of the concentration of NO in kmol/m^{3}in all channels at the outlet section for the laboratory scale wall-flow filter system at 350 °C with reaction and Q = 1017.5 Ncm^3/(min, inlet channel).

The concentration distribution of NO in the different channels helps to understand the following results which describe the molar fraction of NO in the channels for the laboratory scale.

Figure 31 shows the molar fraction in channel 1. The molar fraction of NO is highest at the floor since the flow of NO is entering channel 1 only from channel 10, which is situated right below channel 1. As can be seen in figure 36 the molar fraction decreases from the floor

towards the roof with a minimum in the right corner. The right wall has the lowest molar fraction in the channel due to the distribution of the flow. The bulk has a lower value compare to the floor since all of the flow will go through the porous wall at the floor and react before reaching the bulk. The molar fraction in channel 6 can be explained with the same reasoning since channel 1 and 6 are equal.

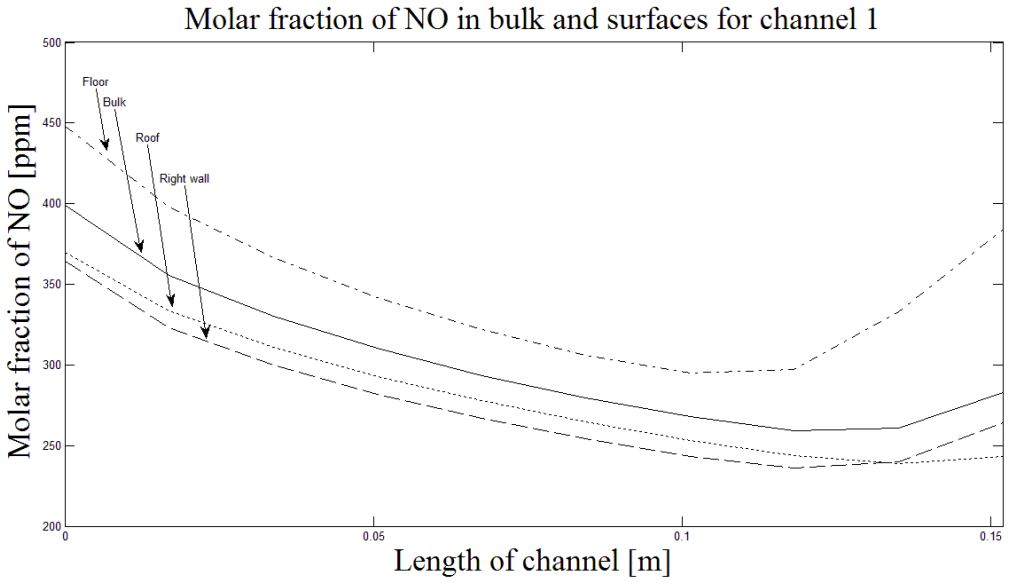

Figure 31. The molar fraction of NO in the bulk and on the surfaces in channel 1, for the laboratory scale wall- flow filter system at 350 °C with reaction and Q = 1017.5 Ncm^3*/(min, inlet channel).*

In channel 10, see figure 32, the top is adjacent to channel 1, the right side to channel 3 and the bottom to channel 5. The three flow-through walls around channel 10 differ since the surrounding channels have different pressure drops and therefore the transport of the flow is not the same. The pressure drop (figure 14) across channel 5 and 10 is the smallest, across channel 3 and 10 it is intermediate and the largest pressure drop is over channel 1. These different pressure drops give rise to different velocity distributions. As mentioned earlier the highest pressure drop is due to that channel 1 only have one flow-through wall compared to channel 3 which have two and channel 5 which have four. The velocity through the porous wall (figure 17) is highest across channel 1 due to the highest pressure drop. The high velocity gives rise to the high molar fraction at the roof. The velocity across channel 5 is the lowest due to the low pressure drop since all walls are flow-through walls and can therefore contribute to the transport of the flow; this leads to the lowest surface concentration at the floor in channel 10. Channel 10 and 12 are equal which makes this explanation valid even for channel 12.

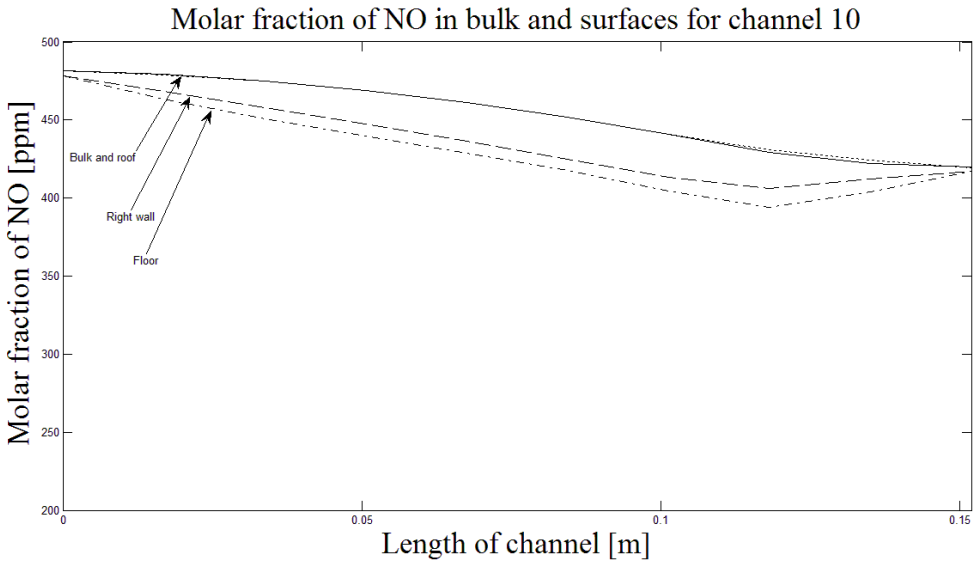

Figure 32. The molar fraction of NO in the bulk and on the surfaces in channel 10, for the laboratory scale wall-flow filter system at 350 °C with reaction and Q = 1017.5 Ncm^3*/(min, inlet channel).*

In channel 3, see figure 33, the molar fraction on the floor and the left wall and also on the roof and the right wall are very similar. This comes from that the flow is homogeneous distributed into the channel from the inlet channels placed at the left wall and the floor. The roof and right wall are adjacent to the cement. Since the flow through the porous wall at the left side should be equal to the porous wall at the floor, the molar fraction on the two surfaces should be the same. The low values at the roof and right wall is due to that these walls are non-flow-through walls and the mass transport is only controlled by diffusion.

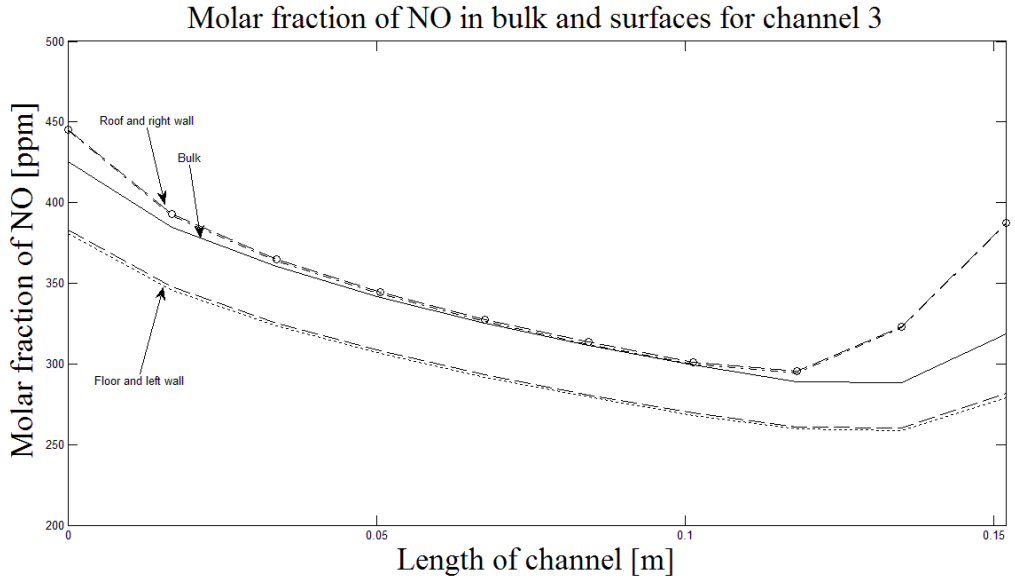

Figure 33. The molar fraction of NO in the bulk and on the surfaces in channel 3, for the laboratory scale wall-flow filter system at 350 °C with reaction and Q = 1017.5 Ncm^3*/(min, inlet channel).*

In channel 5, see figure 34, the molar fraction of NO in the bulk, on the roof and the right wall are very similar. This is expected since the flow from the inlet channels is homogeneously distributed from the roof and the left wall.

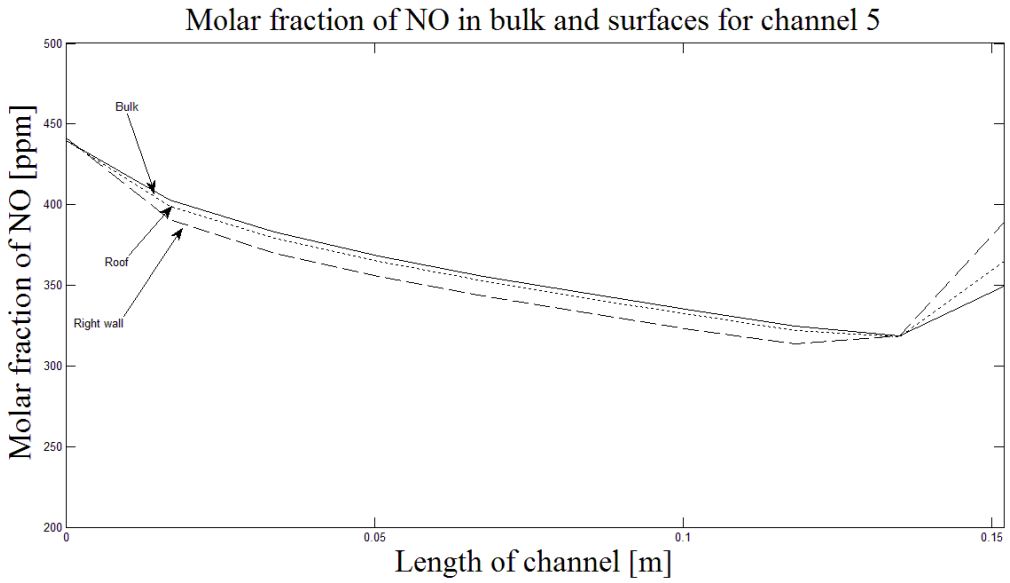

Figure 34. The molar fraction of NO in the bulk and on the surfaces in channel 5 for the laboratory scale wall-flow filter system at 350 °C with reaction and Q = 1017.5 Ncm^3*/(min, inlet channel).*

4.1.6.2 Full scale

In figure 35 the molar fraction of NO on the walls and the bulk in the in- respective outlet channels are shown for the volumetric flow rate 452 Ncm^3/(min, inlet channel). The molar fraction in the bulk for the inlet channels is represented by the solid black line, on the walls in the inlet channels by the black "--" line, in the bulk for the outlet channels by the solid red line and on the walls in the outlet channels by the red "--" line. Towards the outlet section a slightly increase in the molar fraction can be noticed. For the full scale the molar fraction in the bulk phase for the two inlet channels are equal and so is the molar fraction in the bulk phase for the two outlet channels. The same is for the molar fraction of NO on the different walls in the in- respective outlet channels.

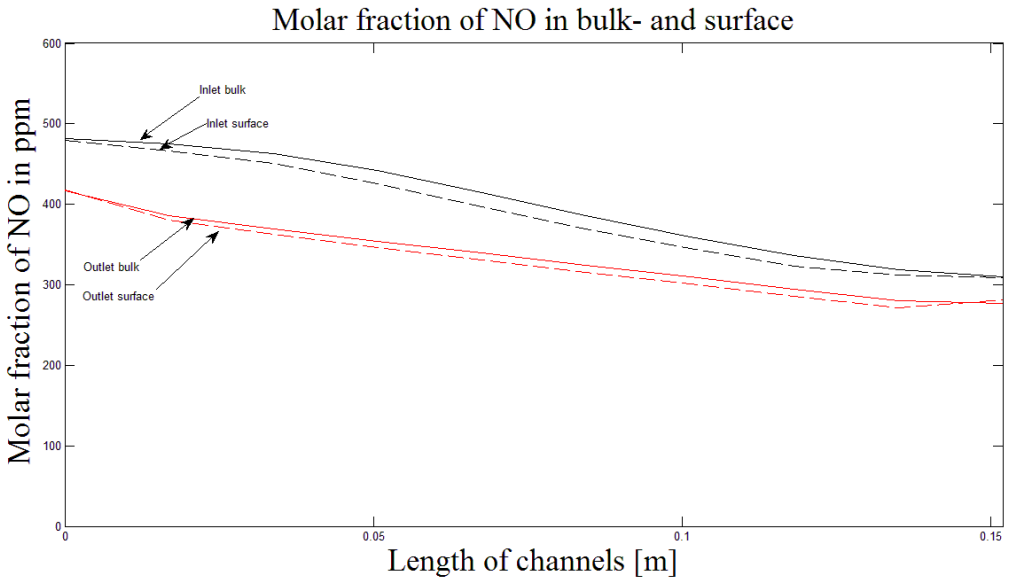

Figure 35. Molar fraction of NO on the surfaces and in the bulk for the full scale wall-flow filter system at 350 ^{o}C with reaction and Q=452Ncm^{3}/(min, inlet channel)

4.1.6.3 Comparison – Laboratory scale and full scale

In figure 36 the molar fraction of NO in the bulk for the inlet channels is shown for the laboratory scale and for the full scale. When the same volumetric flow rate per inlet channel is used for the two scales the molar fraction of NO is the same. This is because in the inlet channels the flow has not passed through the porous wall and no reaction has taken place yet. When the same residence time is used instead the molar fraction of NO in the full scale is decreasing more along the length.

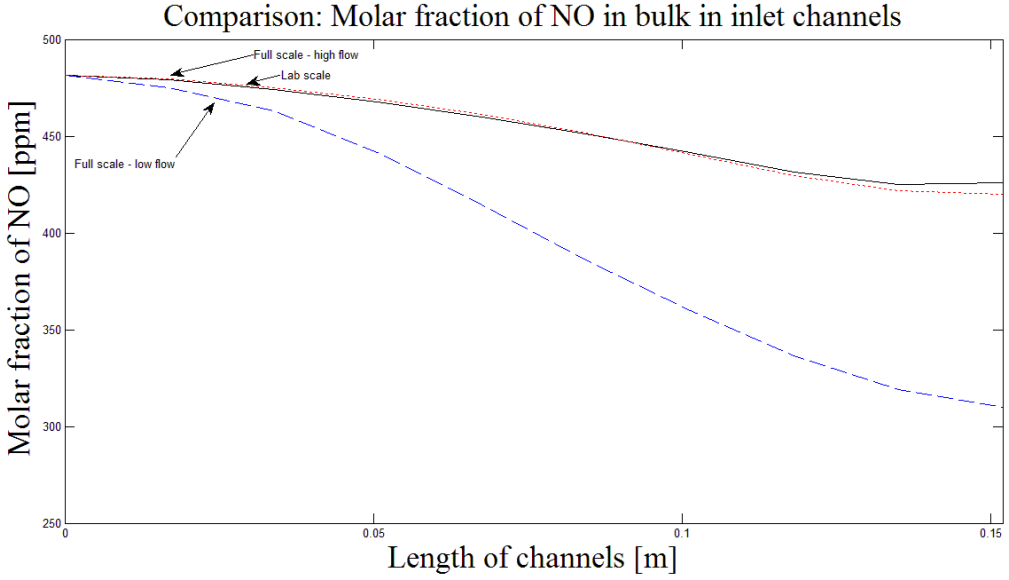

Figure 36. The molar fraction of NO in the bulk in the inlet channels, for full scale with Q= 1017.5 Ncm^{3}/(min, inlet channel), full scale with Q = 452 Ncm^{3}/(min, inlet channel) and laboratory scale with Q= 1017.5 Ncm^{3}/(min, inlet channel), wall- flow filter system at 350 °C with reaction.

In figure 37 the molar fraction of NO in the bulk for the outlet channels is shown for the laboratory scale and for the full scale. When the results for the laboratory scale and the full scale is compared it can be concluded that the molar fraction is higher for the full scale than for the laboratory scale when the same volumetric flow rate per inlet channel is used. This is explained by the higher volume of catalyst in the laboratory scale which gives a longer residence time. When the same residence time is used for the two scales which results in a lower volumetric flow rate per inlet channel for the full scale, the molar fraction of NO in the bulk and on the surfaces is lower for the full scale meaning that more of the reactants have reacted. This result indicates that when the same residence time is used the performance of the reduction of NO is better in the full scale compared to the laboratory scale.

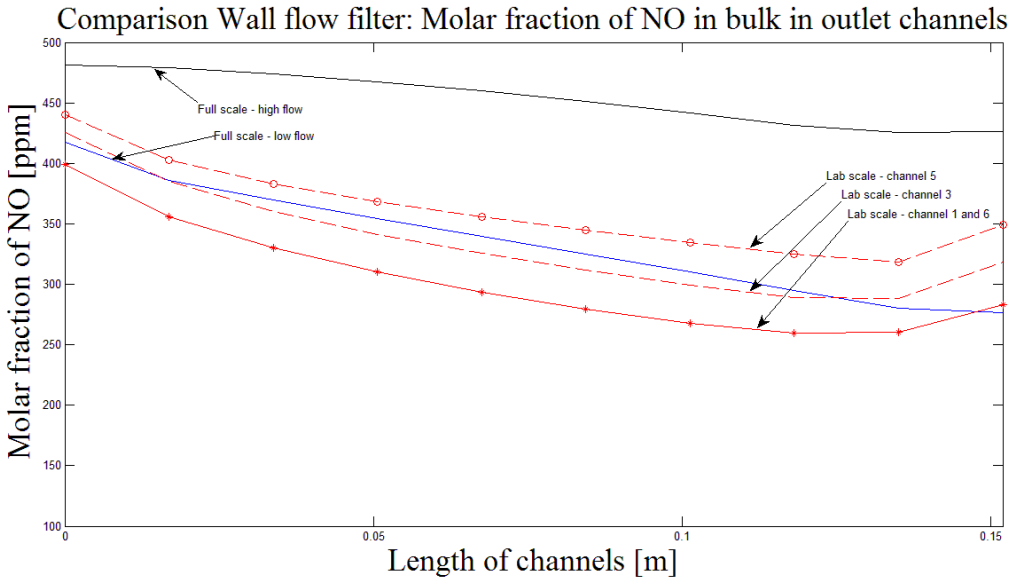

Figure37. The molar fraction of NO in the bulk and in the outlet channels, for the full scale with Q= 1017.5 Ncm^3/(min, inlet channel), the full scale with Q = 452 Ncm^3/(min, inlet channel) and the laboratory scale with Q= 1017.5 Ncm^3/(min, inlet channel), wall- flow filter system at 350 °C with reaction.

When the molar fraction at the surface is studied for the flow-through walls respectively the non-flow-through walls for the laboratory scale a difference between the two types of walls is observed. The non-flow-through walls have a higher surface concentration, but still the surface concentration on the flow-through walls decreases along the length of the channel. This behavior indicates that all walls are participating in the NO reduction even though the flow-through walls have a larger contribution.

An interesting thing to point out is that the molar fraction of NO is increasing towards the outlet section in the outlet channels, and this can be observed in both the laboratory scale and the full scale. To confirm that this increase does not have to do with velocity changes the mole flow of NO was studied. The same behavior is observed even in these graphs; see section 4.1.7. molar flow of NO.

4.1.7 Molar flow of NO

Figure 38 and 39 show the molar flow of NO in the outlet channels for the laboratory scale respectively the full scale for the same residence time. This result confirms that the molar fraction of NO actually increases in the outlet section. As have been discussed before the

pressure drop increases towards the outlet section and thereby also the velocity through the porous wall. This behavior was even more significant in the laboratory scale with reversed channels. Due to this velocity acceleration the contact time between the reactants and the catalytic material is lower in this region. The amount of NO that passes the porous wall without taking part in the reaction is higher and the mole flow of NO is increased. This behavior affects the conversion of NO in a negative way. The conversion that is being measures in the end of the channels is actually not the highest reached conversion. The highest conversion is instead reached before the velocity through the porous wall starts to increase. However, when the filter starts to be filled with soot the pressure drop is likely to decrease in the outlet section and the effect with the increased molar flow of NO will not be so significant.

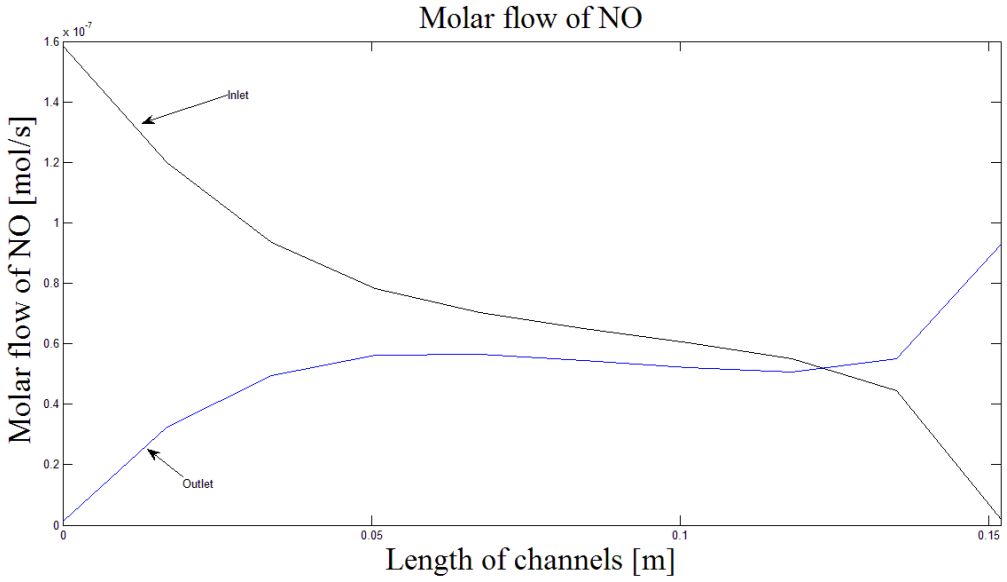

Figure 38. The molar flow of NO in the bulk for the full scale with Q= 452.5 Ncm^3/(min, inlet channel), wall- flow filter system at 350 °C with reaction.

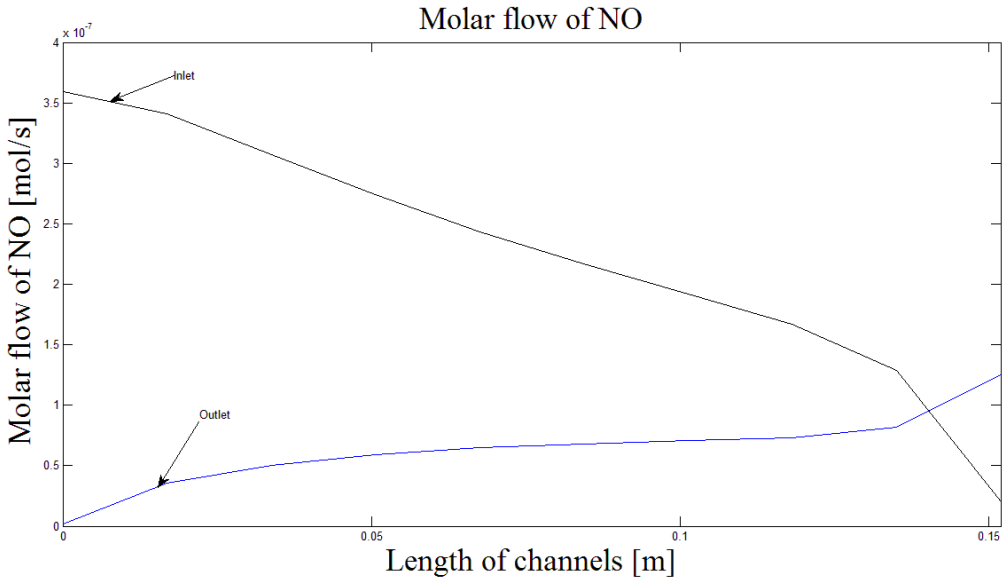

Figure 39. The molar flow of NO in the bulk for the laboratory scale with Q= 1017.5 Ncm^3/(min, inlet channel), wall- flow filter system at 350 °C with reaction.

4.1.8 Conversion of NO

Figure 40 shows the conversion of NO for the laboratory scale and the full scale. For the full scale the conversion of NO is shown for the two volumetric flow rates 1017.5 Ncm^3/(min, inlet channel) respective 452 Ncm^3/(min, inlet channel). The volumetric flow rate 1017.5 Ncm^3/(min, inlet channel) is used for the laboratory scale.

The highest conversion is observed for the full scale when the volumetric flow rate 452 Ncm^3/(min, inlet channel) is used. This means that when the same residence time is used for the full scale and laboratory scale the conversion is higher for the full scale. This is an effect of the non-flow-through walls that are present in the laboratory scale. The lowest conversion is received for the full scale when the same volumetric flow per inlet channel is used as for the laboratory scale meaning 1017.5 Ncm^3/(min, inlet channel). Since the volume of catalyst per inlet channel is lower for the full scale the residence time will be shorter if the same flow per inlet channel is used. Therefore it is not suitable to feed the same volumetric flow per inlet channel for the full scale and laboratory scale if a fair comparison between the conversions should be done.

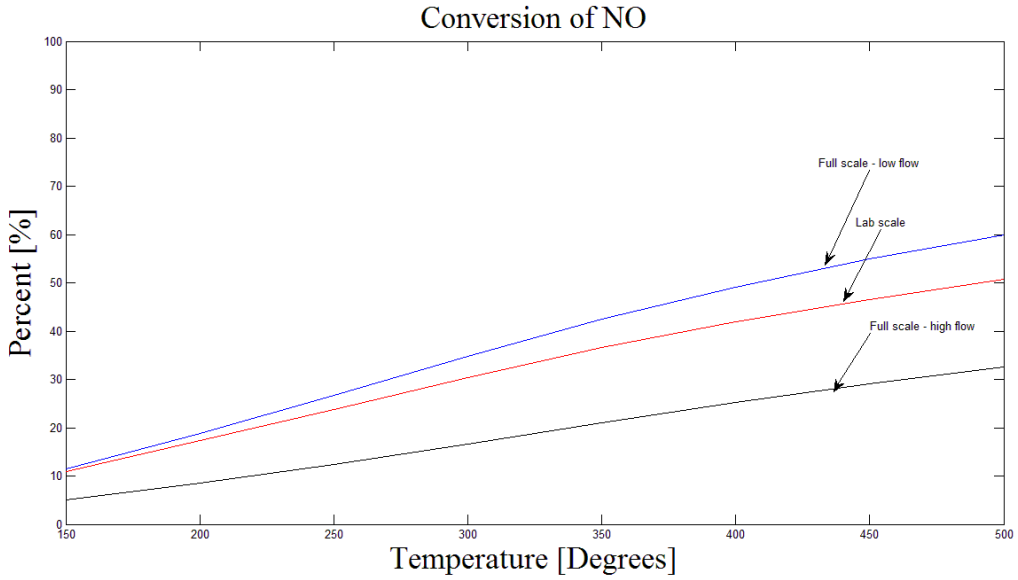

Figure 40. Conversion of NO for the full scale with Q=1017.5 Ncm^3/(min, inlet channel)and Q=452 Ncm^3/(min, inlet channel) and for the laboratory scale for Q=1017.5 Ncm^3/(min, inlet channel).

4.2 Monolith system with reaction

In the monolith configuration the total volumetric flow 4070 Ncm^3/min is used for the laboratory scale which is the same as the 1017.5 Ncm^3/(min, inlet channel) origins from. However, in the monolith case for the laboratory scale the total flow is divided by 13 inlet channels instead of four. This gives a lower volumetric flow per inlet channel, but the residence time will remain the same since it is the same flow fed to the same volume of catalyst. The same adjustment as before is done for the full scale so the residence time will be the same as for the laboratory scale. In the monolith case the transport through the porous wall is negligible since this transport is only controlled by diffusion.

4.2.1 Pressure profiles

In figure 41 the static pressure in the channels is presented for the monolith case for the laboratory scale and the full scale. For the monolith case there are no in-respective outlet channels so the pressure profiles are the same for all channels. The higher static pressure in the laboratory scale compared to the full scale comes from the different volumetric flow rates.

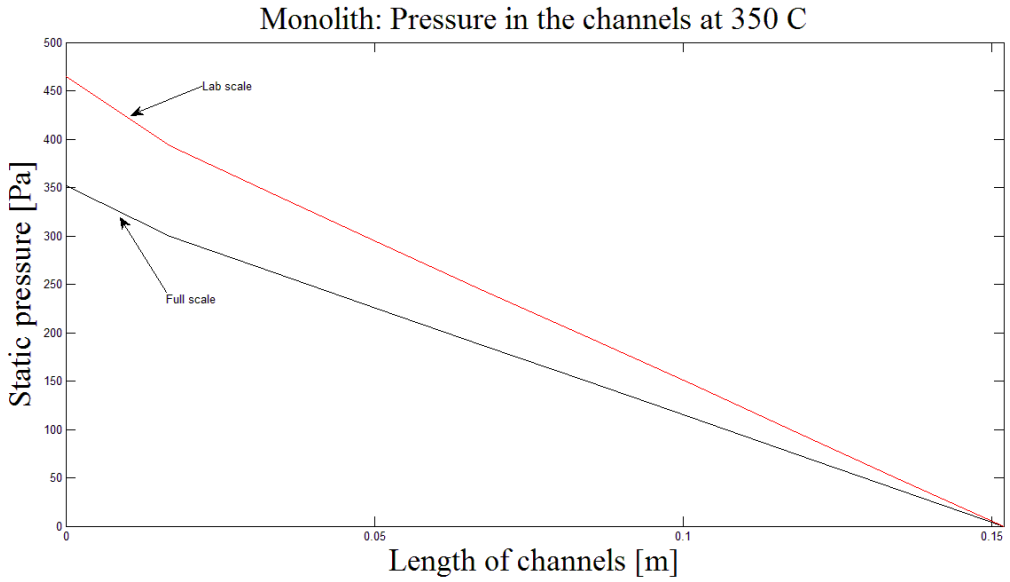

Figure 41. The static pressure along the length of the channels for the full scale with Q= 225.7 Ncm^3/(min, inlet channel and the laboratory scale with Q= 313.1 Ncm^3/(min, inlet channel), monolith system at 350 °C with reaction.

4.2.2 Velocity profiles

Figure 42 shows the velocity in the channels for the full scale and laboratory scale. The difference in velocity between the two scales is due to the different volumetric flow rates to receive the same residence time. The small acceleration in the beginning of the channels is the result of the development of a fully developed flow.

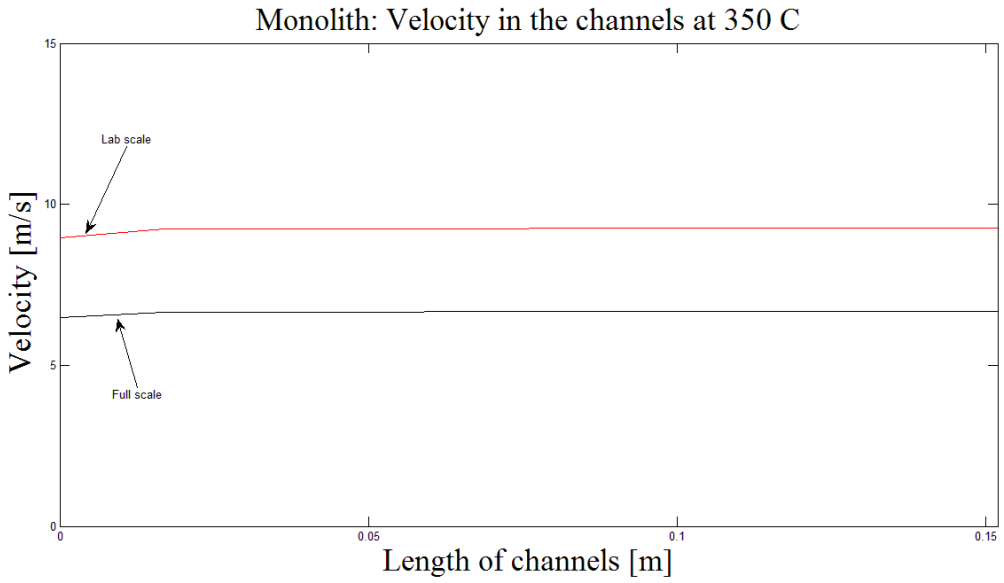

Figure 42. The velocity along the length of the channels for the full scale with Q= 225.7 Ncm^3/(min, inlet channel and the laboratory scale with Q= 313.1 Ncm^3/(min, inlet channel), monolith system at 350 °C with reaction.

For the monolith case the velocity in four points, in a cross sectional plane in one channel was measured. The ratio between the velocity in every point and the maximum velocity in the cross sectional plane was calculated (see figure 12). These ratios are compared with the theoretical values for a monolith system. The ratio from the simulations, the theoretical values and the percentage differences are given in table 7. The highest percentage difference between the measured velocity and the theoretical is found in point 3, which has the longest distance to the center. The closer the measured point is to the center and maximum velocity, the lower is the percentage difference to the theoretical ratio. The higher difference farther away from the center might be due to that the theoretical model does not take into account the secondary flow in the corners while this phenomenon is included in the simulations.

Table 7. The ratio of U/U_{max} , simulated and theoretical values for a monolith case.

Laboratory scale				
U/U_{max} simulation	0.9232	0.6143	0.5720	0.3956
U/U_{max} theoretical	0.9038	0.5925	0.5418	0.3703
Percentage difference	2.14	3.67	5.56	6.83
Full scale				
U/U_{max} simulation	0.9088	0.6353	0.5834	0.4204
U/U_{max} theoretical	0.9038	0.5925	0.5418	0.3703
Percentage difference	0.54	7.22	7.67	13.52

4.2.3 Molar fraction of NO

In figure 43 the molar fraction of NO in the bulk phase is shown for the full scale and the laboratory scale with the same residence time. Even in the monolith case a difference between the laboratory scale and the full scale can be observed. Like for the wall-flow filter case the

reduction of NO is higher for the full scale. This confirms that there is a mass transport resistance in the laboratory scale which is not present in the full scale.

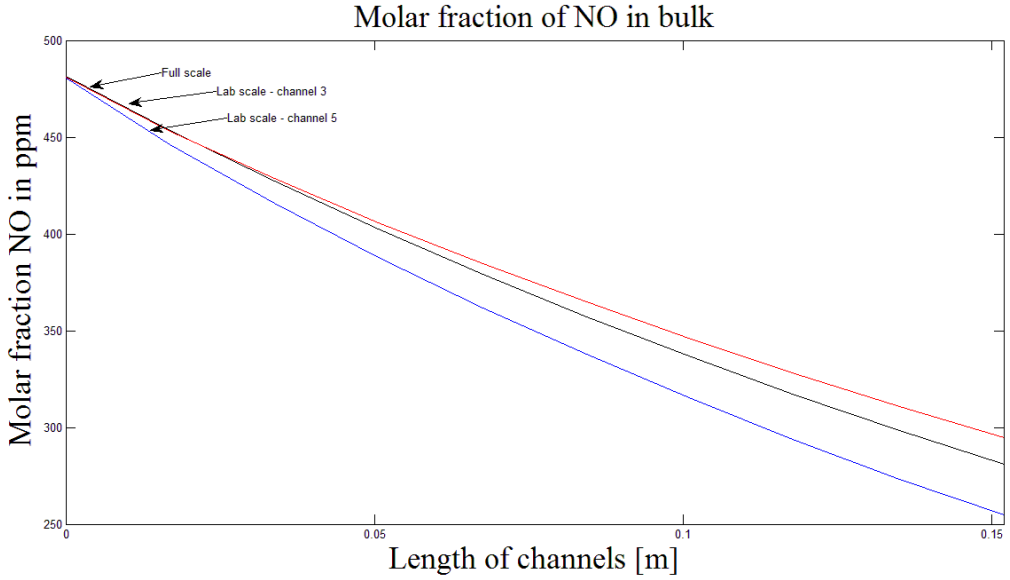

Figure 43. The molar fraction of NO in the bulk for the full scale with Q= 225.7 Ncm^3/(min, inlet channel) and the laboratory scale with Q= 313.1 Ncm^3/(min, inlet channel), monolith system at 350 °C with reaction.

Figure 44 shows the molar fraction of NO at the surfaces for the full scale and laboratory scale. In the monolith case the flow is not forced through the flow-through walls, but instead the motion of the flow is controlled by diffusion for all walls. Still there is a difference between the flow-through walls and the non-flow-through walls. Why there is a difference between the molar fractions in the inlet section between the channels cannot be explained at the moment.

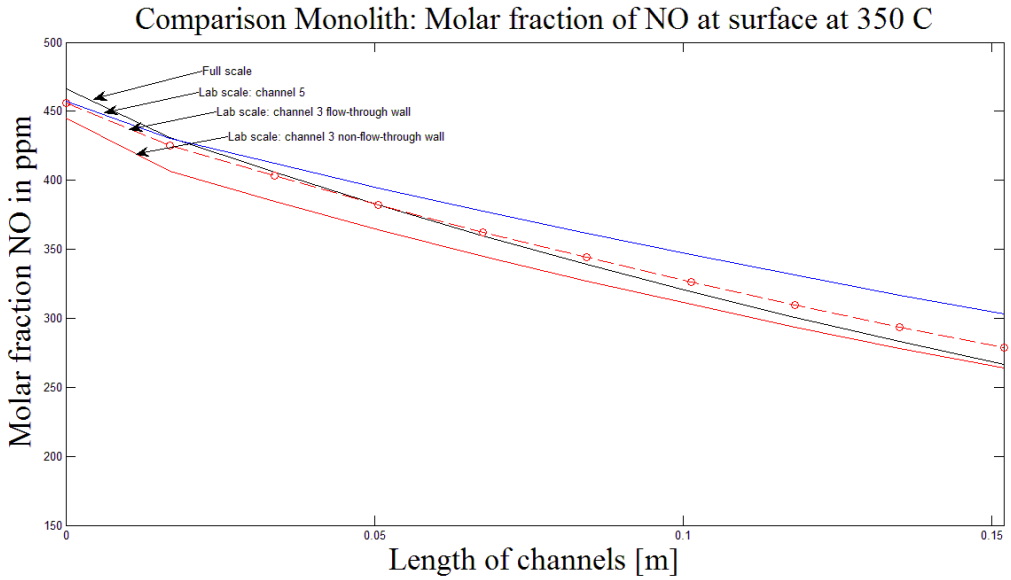

Figure 44. The molar fraction of NO at the surfaces for the full scale with Q= 225.7 Ncm^3/(min, inlet channel) and the laboratory scale with Q= 313.1 Ncm^3/(min, inlet channel), monolith system at 350 °C with reaction.

To study the influence of the non-flow-through walls the molar fraction of NO through the porous wall was investigated. In figure 45 the molar fraction of NO through the porous wall is shown for the full scale and the laboratory scale. For the laboratory scale the two different kinds of walls are presented. The full scale is represented by the blue line, the flow-through walls in the laboratory scale by the black line and the non-flow-through-walls in the laboratory scale by the red line.

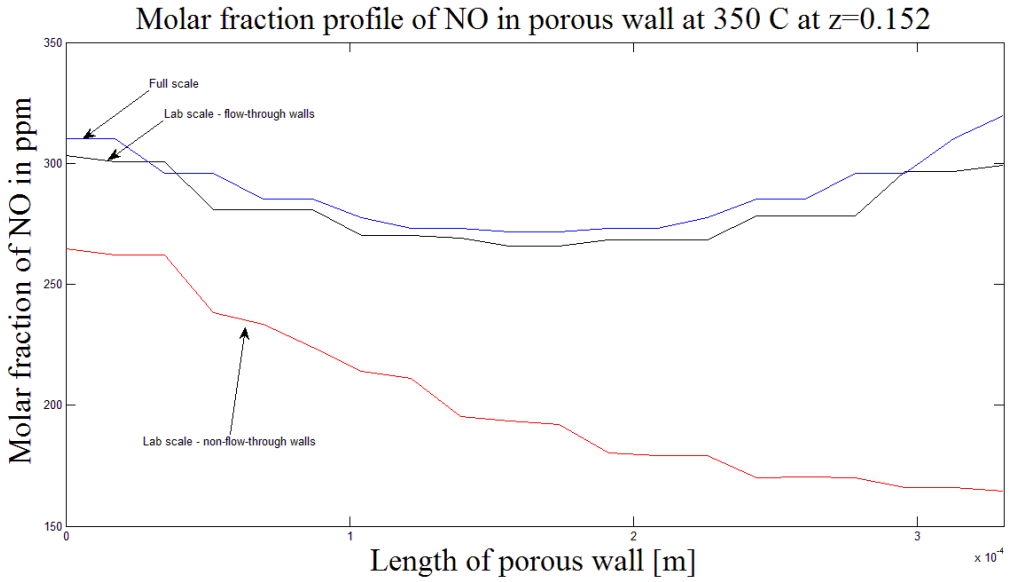

Figure 45. The molar fraction of NO through the porous wall for the full scale with Q= 225.7 Ncm^3/(min, inlet channel) and the two different walls in the laboratory scale with Q= 313.1 Ncm^3/(min, inlet channel), monolith system at 350 °C with reaction.

As can be seen in the figure there is a significant difference in the molar fraction of NO in the porous wall between the flow-through walls and the non-flow-through walls. The molar fraction profile for the flow-through walls is rather flat while a significant gradient is observed for the non-flow-through walls. The profile for the porous walls in the full scale and the flow-through walls in the laboratory scale are almost equal which is expected since these walls are identical. The flow-through walls have channels on both sides and due to this the diffusion occurs from both sides towards the center. This gives the U-shaped behavior for the concentration profile through the porous wall. The non-flow-through walls have only channels on one side; this increases the transportation length for the reactants. The reactants have to be transported through the entire thickness of the porous wall, and thereby the distance will be doubled compared to the flow-through walls. This creates an internal mass transport resistance. The difference in conversion of NO between the full scale and the laboratory scale can be explained by the presence of the non-flow-through walls in the laboratory scale and thereby the diffusion limitations in the non-flow-through walls. To study if the mass transport resistance is due to diffusion limitations both the internal and external mass transfer resistance is removed for the laboratory scale. Figure 46 shows that there is now no concentration gradient in the porous wall and there is no difference between the molar fraction of NO for the flow-through-walls and non-flow-through walls in the laboratory scale. This confirms that it actually is a mass transport resistance due to diffusion limitations in the non-flow-through walls.

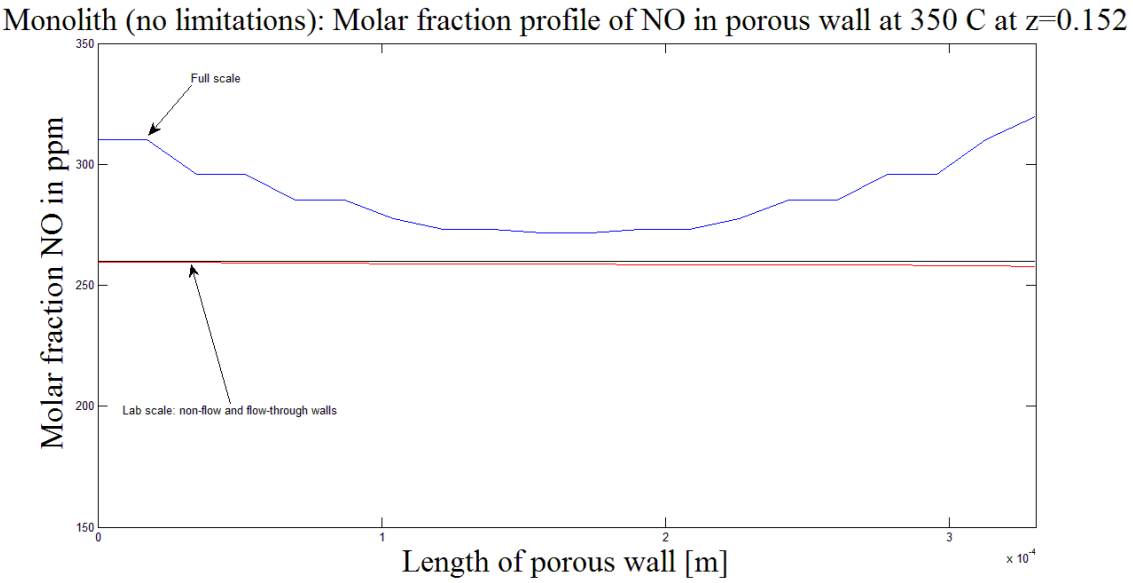

Figure 46. The molar fraction of NO through the porous wall for the full scale with Q= 225.7 Ncm^3/(min, inlet channel) and the two different walls in the laboratory scale with Q= 313.1 Ncm^3/(min, inlet channel), monolith system with no diffusion limitations in the laboratory scale at 350 °C with reaction.

4.2.4 Conversion of NO

In figure 46 the conversion of NO is shown for the full scale and the laboratory scale for the monolith case. Just as in the wall-flow filter case the full scale has a higher conversion of NO than the laboratory scale when the same residence time is used. This is due to the diffusion limitations that were discussed above. The diffusion limitations are more significant at high temperatures. At high temperatures, the reaction rate will increase more rapidly than the diffusion rate and due to that the significance of the diffusion limitations increases with increased temperature.

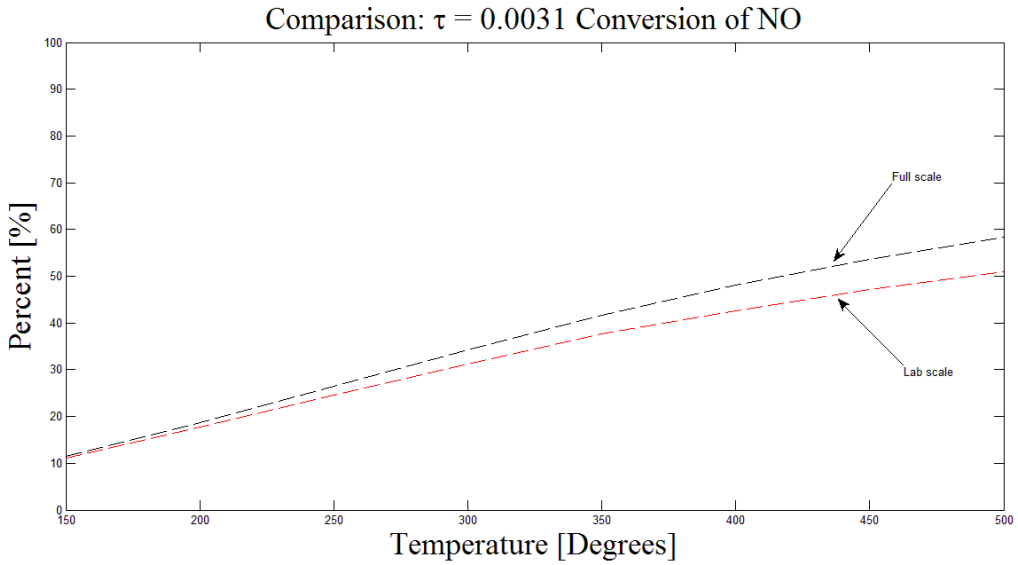

Figure 47. Conversion of NO for the full scale with Q=225.7 Ncm^3/(min, inlet channel) and for the laboratory scale for Q=313.1 Ncm^3/(min, inlet channel) for a monolith system.

4.3 Comparison between the wall flow filter and monolith configuration

In figure 48 a comparison between the wall-flow filter system and the monolith system for the conversion of NO for the laboratory scale and the full scale is shown.

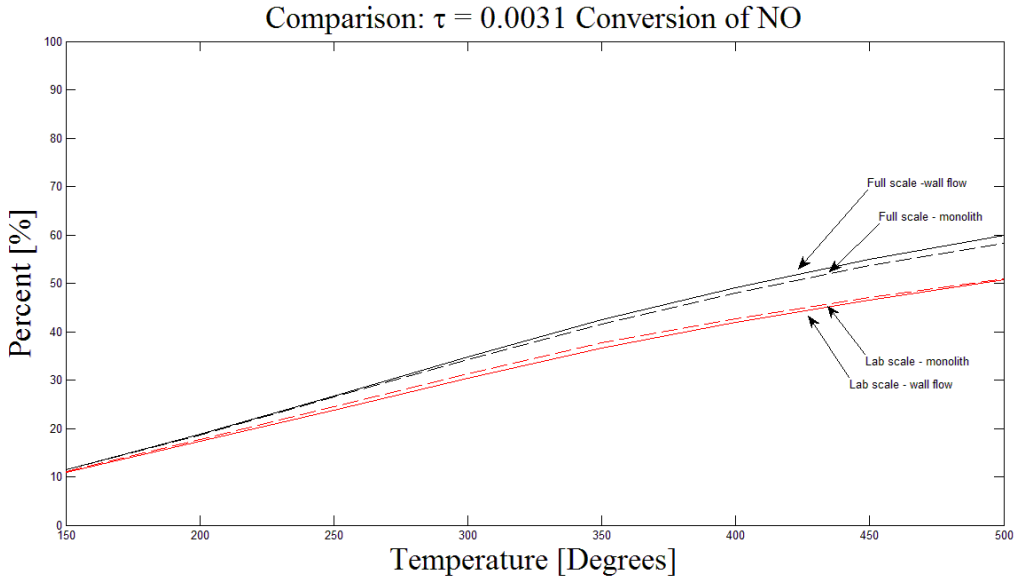

Figure 48. Conversion of NO for the full scale with Q=225.7 Ncm^3/(min, inlet channel) and for the laboratory scale for Q=313.1 Ncm^3/(min, inlet channel) for a wall-flow filter system and monolith system.

For the laboratory scale the monolith system and the wall-flow filter gives almost the same conversion of NO, and the same situation is for the full scale. This result indicates that under these conditions there is actually no difference in the effectiveness of NO reduction between the two configurations. It seems like it does not matter how the gas contacts the catalyst, the performance of the NO conversion is still the same. This also explains why the permeability has no or low impact on the NO conversion. Even though there is no difference in the NO conversion between the wall-flow filter and the monolith there is a difference between the laboratory scale and the full scale when it comes to the conversion of NO. This result has already been discussed and is explained by mass transport limitations.

In this case a low value for the activation energy has been used; if a higher value for the activation energy would have been used instead an even higher difference between the laboratory scale and full scale would have been observed. At 500 ^{o}C a difference between the conversion for the monolith and wall-flow filter starts to appear for the full scale; this difference is also expected to increase at higher temperature if a higher value for the activation energy should be used. The monolith configuration is then expected to give a lower conversion than the wall-flow filter due to diffusion limitations in the monolith configuration.

The difference in NO conversion between the laboratory scale and full scale indicates that the non-flow-through walls have a major impact on the results. The effect of internal mass transport resistance is significant for the non-flow-through walls in the laboratory scale. The Thiele module and the effectiveness factor do not give a clear answer that there are diffusion limitations in the non-flow-through walls and no such limitations in the flow-through walls,

but the calculated values points in this direction and show that there is a difference between the two types of walls.

4.4 Quality control

In this section the quality of the results is investigated by checking convergence criteria and the mesh quality.

4.4.1 Convergence

The convergence criteria have been checked with mass imbalance, scaled residuals and comparison of molar/mass fractions. The simulations are considered converged when mass imbalance is lower than $1 \cdot 10^{-15}$, the scaled residuals are lower than $1 \cdot 10^{-7}$ and the ration between mass flow in and out of the channels is lower than $1 \cdot 10^{-7}$.

4.4.2 Mesh quality

The mesh quality is given in table 8 for laboratory and full scale case.

Table 8. Mesh quality for laboratory and full scale case.

	Laboratory scale	**Full scale**
Skewness	0.45	-
Aspect ratio	22	10
Number of cells	~1 million	~1.2 million

5. Overall discussion

In the NH_3-SRC system there is a network of reactions, but in this project only the standard SCR-reaction has been considered. This approximation can be done when NO and NH_3 oxidation do not occur. The oxidation phenomenon is dependent on the residence time but might start at approximately 300 ^{o}C. Nevertheless, the oxidation is considered to have low impact on the results. The purpose with this project is to see this as a model reaction and not to investigate the SCR reaction network and therefore this approximation is justified. It is also possible to run the simulations at steady state conditions, as has been done in this project. If there would have been NO_2 in the feed gas transient simulations would have been required.

When it comes to quality of the mesh it is always possible to refine the mesh to get better solutions. In this project the comparison between the laboratory scale and full scale has been the important matter, and since the mesh is equivalent for the two cases the comparison is fair. However, if the absolute values from the simulations are of interest to study a refinement of the mesh might be of importance.

The geometry used for laboratory scale is not the smallest possible geometry to model in Fluent. By the use of symmetry planes the smallest possible geometry is 1/8 of the total volume, this was also done as a first approach. However, this approach gave unreliable results in the channels where symmetry where used, therefore 1/4 of the total volume was used instead. The problems might be due to the fact that some channels where divided on the

diagonal. Nevertheless, the simulations where 1/8 of the volume is used should be possible and a deeper study of these problems must be done to identify the reason to the problems.

Three different convergence criteria have been used in this project, the difference between the mass in the inlet and in the outlet, the scaled residuals and mass imbalance. The convergence criteria that have been used are low and the results are not likely to change if they are defined even lower. Instead if higher accuracy of the results is needed efforts to refine the mesh should be done. To shortening the simulation time it could be possible by increasing the convergence criteria.

6. Conclusions

The main conclusion from this project is that there are differences between the laboratory scale and the full scale, and caution must be taken if the results from the laboratory scale should be transferred to the full scale. The main differences are the ratio between inlet and outlet channels, the volume of catalyst per inlet channel and the impact of the non-flow-through walls due to diffusion limitations in the laboratory scale.

Since the ratio between the inlet and outlet channels is not the same the absolute values of the static pressure and the velocity in the channels are difficult to compare. The different volume of catalyst makes it not suitable to use the same volumetric flow rate per inlet channel in the two different scales if a fair comparison between the conversions should be made. All walls in the laboratory scale participate in the reaction, even if the non-flow-through walls do not contribute in the same extent as the flow-through walls. The reaction is controlled by diffusion limitations in the non-flow-through walls in the laboratory scale which gives a negative impact on the NO conversion since they contribute to an underestimation of the conversion. An increase in the mole flow of NO was observed in the outlet channels towards the outlet section for both scales for the wall-flow filter configuration; this is caused by the increased pressure drop and velocity through the porous wall in this region. This behavior has a negative impact on the NO conversion.

When the temperature is increased the velocity, static pressure and conversion increase as well. The permeability has an influence on the velocity and static pressure but only a low impact on the NO conversion. When Darcy's law is used to model for the porous wall the porosity will not have any impact on the velocity, static pressure or the NO conversion.

7. Future studies

In future studies it would be interested to study the complete SCR reaction system to investigate which affects this may have. It would also be interested to study a non-uniform distribution of the catalyst to see how the efficiency in the reduction of NO is controlled by the distribution. It would also be of great interest to further study the effect of diffusion limitations in non-flow-through walls.

References

[1] Soldati et.al (2005) Appraisal of three-dimensional numerical simulation for sub-micron particle deposition in a micro-porous ceramic filter. Chemical Engineering Science vol 60 pp 6551 – 6563

[2] Caldirola F., De Leo F. (2009) *Experimental and modeling study of the NH_3-SCR reactions over a catalyzed wall – flow filter for the after treatment of diesel exhausts.* Milano: Politecnico di Milano (Mater thesis at Energy Department - Laboratory of Catalysis and catalytic processes)

[3]S. Redaelli (2010) *Experimental and modeling study of the NH_3-SCR activity in a catalyzed wall-flow diesel particulate filter*. Milano: Politecnico di Milano. (Power point presentation at Department of chemistry, chemical engineering and materials)

[4] London A. L. (1978) *Laminar flow forced convection in ducts.* London: Academic Press INC.

[5] Andersson, Bengt et al (2010) *Computational Fluid Dynamics for Chemical Engineers,* sixth edition. Göteborg.

[6] ANSYS Fluent (2006) *Setting Dynamic Mesh Modeling Parameters.* Fluent 6.3 User's guide chapter 11.7.1 (2011-02-25)

Appendix A
Parameter explanation

Explanation and units to the parameters in equations (1) – (17)

Parameter	Explanation	Unit
A	Pre-exponential factor	-
a	Half width of channel	m
α	Permeability	m^2
b	Half height of channel	m
C	Concentration	mol/m^3
Cp	Specific heat capacity	J/K
c_1	Pressure gradient	1/m, s
D	Diffusion coefficient	m^2/s
g	Gravitational force	m/s^2
ΔH	Reaction enthalpy	J/mol
k_{eff}	Conductivity constant	W/m·K
k_0	Reaction rate constant	1/s
L_{diff}	Diffusion length in catalyst	m
η	Effectiveness factor	-
η_{NO}	Conversion of NO	%
ϕ	Thiele module	-
P	Pressure	Pa
ρ	Density	kg/m^3
t	Time	s
T	Temperature	K
τ	Residence time	1/s
τ_{kj}	Stress tensor in eq. (X)	N/m^2
U and u	Velocity	m/s
u_{max}	Maximum axial velocity across the duct cross section	m/s
x	Coordinate	m
x_{cat}	Fraction of catalyst in the porous wall	%
xo_{NO}	Mass fraction of NO in inlet section	%
x_{NO}	Mass fraction if NO in outlet section	%
y	Height coordinate	m

Appendix B

Kinetic parameters

In this section the values for the parameters in the reaction rate for the standard SCR reaction are presented.

Table B.1 Values for the kinetic parameters obtained by fitting standard SCR reaction powder runs

Parameter		Value	Unit
	Rate constant	4.876025	1/s
	Activation energy	21658.3872	J/mol
	Catalyst load	0.089357	%
	Reference temperature	573.15	K

Appendix C

Technical information in laboratory scale

The figures shows the geometry for the laboratory scale modeled in Fluent, corresponding to one fourth of the total geometry for laboratory scale.

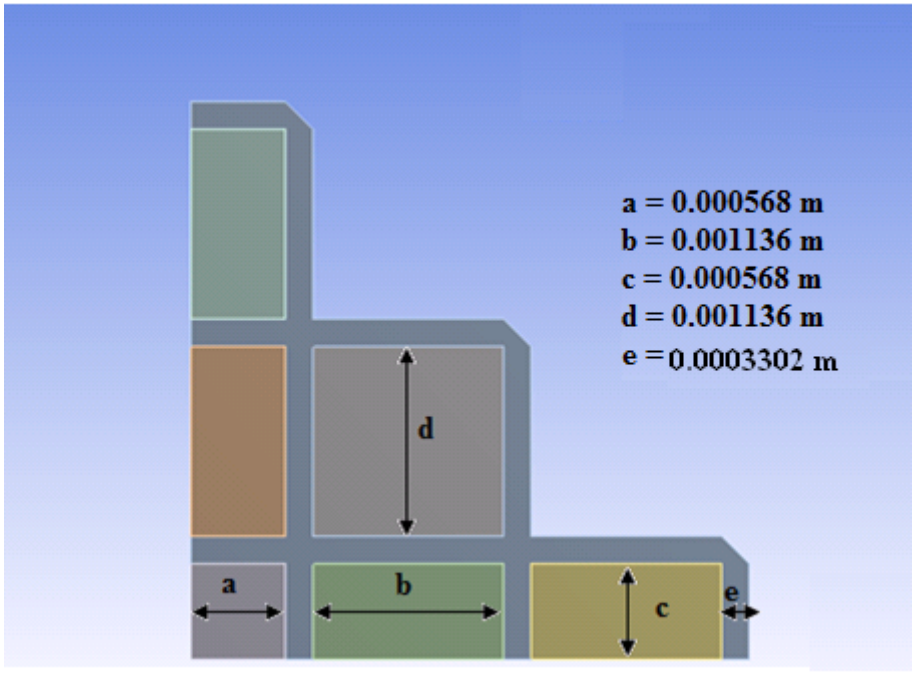

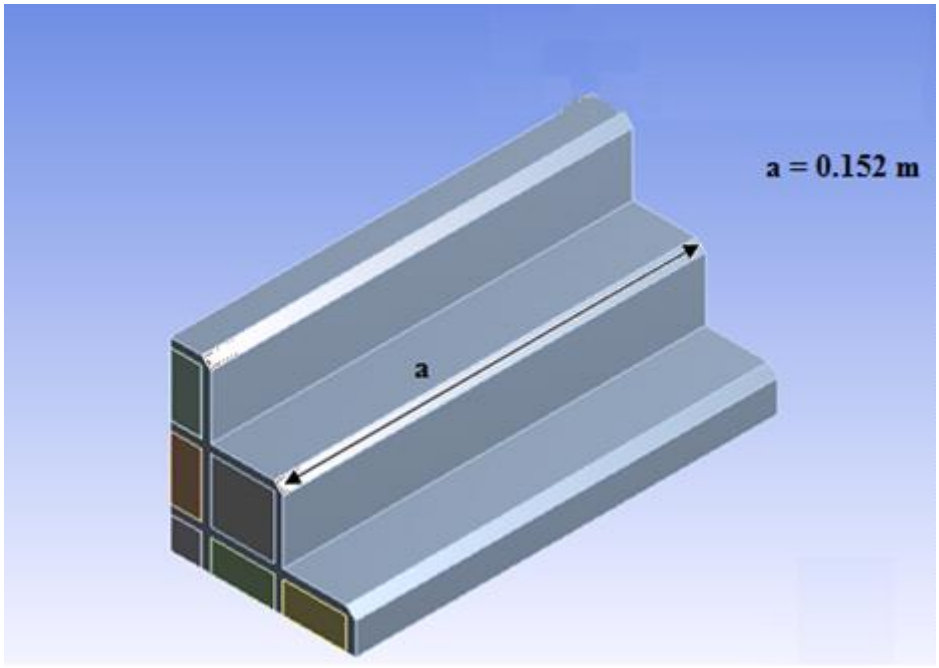

Appendix D

Technical information in full scale

The figures show the geometry for the full scale modeled in Fluent. Each channel modeled corresponds to one fourth of a total channel.